Next-generation 3D displays
computer generated holography and speckle reduction

van der Meulen, R.

Award date:
2005

Next-generation 3D displays: Computer Generated Holography and speckle reduction

R. van der Meulen

September 2005
EPG 05-13

Abstract

Within Philips there is a common technique to display 3D information. This is done by using lenticular based displays. For future activities other methods to display 3D information have to be explored as well. Holography is one of those alternative methods to display 3D images. This graduation project is done to find out the strengths and weaknesses of computer generated holography. Therefore the basics of computer generated holography are explored.

An algorithm is created to calculate a hologram to be displayed at a micro-display panel. Given a black and white 3D input file, this algorithm can transform the input image to a hologram using a Fresnel Zone Plate for each white pixel. Due to the amount of pixels on the micro-display panel these calculations take a lot of time. Therefore some time-reducing methods are explored and some of them also implemented. For example a cosine look-up table can be used. Then a array is filled with the values of the cosine. The arguments are divided in equal steps between 0 and 2π. In stead of calculating the cosine function it can be looked-up in this pre-filled array which saves time. Another method to save time is to use the same Fresnel Zone Plate for all the points at one z-distance. Translating in (x, y) of this pattern is the only action which has to be taken. Some further computation time can be gained by substituting the square root function by a Fresnel approximation. For calculating the Fresnel Zone Plate a couple of recurrent formulas can be used to prevent calculating the radius between a display pixel and the object point over and over again. At processor level the square root takes a lot of steps to be calculated whereas summations are much faster. A fourth way of reducing calculation time is to remove the vertical parallax. What is left then is holographic imaging in the horizontal direction and projection imaging in the vertical direction. The Fresnel Zone Plate does not have to be calculated for 2 dimensions anymore, but only for a horizontal line (1 dimension).

Different sorts of holograms exist like phase or amplitude holograms, which can be divided into one of the following three sorts. First the on-axis holograms where the reference beam and object beam are perpendicular to the normal of the micro-display panel. Second the off-axis holograms where either the reference beam or the object beam has a certain angle with the normal of the micro-display panel. Third, the Horizontal Parallax Only (HPO) holography, resulting in holography in horizontal direction and projection in the vertical direction.

The written algorithm is adaptable to calculate holograms for these three sorts of holography. A set-up is built which can be changed to display these three sorts of holograms. This set-up uses a Liquid Crystal on Silicon (LCoS) micro-display panel, whose pixels affects the amplitude of the light when used in combination with a polarizer. Using lenses or a divergent reference beam can change the distance and size of the created image. These effects are measured and they obey the laws for ideal lenses.

One of the problems discovered during the project is the small viewing angle. To enlarge this angle one would like to generate an object to the panel as close as possible. However, creating an object close to the panel means large diffraction angles for the pixels at the edge of the panel. To be able to reach these large angles, the fringes have to be very close to each other. In practice there is a minimum distance: the pixel pitch.
In spite of the fact that holography offers all the depth cues, there are more major disadvantages. These disadvantages will be outlined below. The micro-display panels are too small: more pixels enable the small details to be displayed at the panels as well. The pixel pitch is too large: this pitch determines the size of the smallest details so a smaller pitch makes it possible to display smaller fringes. The use of only one color: only a red laser was available having trouble with uniformity as an extra handicap. The higher order disturbance: due to the pixel structure a lot of higher order images are created next to the desired image. The zeroth order effect: there is a part of the light that goes through the set-up unaffected. This results in a clear background full of speckle surrounding the desired image. The large calculation times and high data rates make it impossible to generate real-time conversions from a scene to a hologram. Due to all the disadvantages mentioned above holography cannot be implemented as a 3D-display technique at this moment.
Another part of the project consisted of reducing the speckle caused by using a diode laser as the light source. Mirror wobbling, mode scrambling and overcoming the coherence length of the laser are all appropriate methods to reduce speckle. To be able to use the de-speckled light for projection purposes a homogeneous light distribution is required, which has been accomplished by using a rod integrator. This is a small bar made out of glass with a partly transparent mirror on one side and a mirror with a pinhole in it at the other side. When the light enters this waveguide through the pinhole 69% of it will come out at the other end reducing the speckle modulation depth from 5.5% to 2.7%. When using the rod integrator the other speckle reduction mechanisms do not result in an even lower speckle modulation depth, so the coherence length is overcome by the integrator.

Contents

1 Introduction **5**

2 Properties of waves **9**
2.1 Waves 9
2.2 Interaction of light waves 10
2.2.1 The principle of superposition 10
2.2.2 Huygens' wavelets 11
2.3 Interference 12
2.3.1 Young's double slit interference experiment 14
2.4 Diffraction 16
2.4.1 Single slit 16
2.4.2 Rectangular aperture 17
2.5 Gratings 17

3 Holography **21**
3.1 Object and reference waves 21
3.2 Fresnel Zone Plate 22
3.3 Point source summation 23
3.4 Phase versus amplitude hologram 24
3.5 Off-axis holograms 24
3.6 Horizontal parallax only 25

4 Displays **27**
4.1 Liquid crystal 27
4.1.1 The liquid crystal variable retarder 28
4.1.2 The liquid crystal display 28
4.1.3 Liquid crystal on silicon 30

5 Speckle **31**
5.1 Laser diode 32
5.1.1 Light versus current 33
5.2 Speckle formation 34
5.2.1 Intensity statistics 34
5.2.2 Speckle sizes 35
5.3 Speckle reduction methods 38
5.3.1 Mirror wobbling 38
5.3.2 Mode scrambling 38

5.3.3 Rod integrator 39

6 Experimental Set-up **43**
6.1 Set-up for displaying Computer Generated Holograms 43
6.2 Set-up for speckle reduction 46

7 Results **49**
7.1 Pixel structure of the LCoS panels 49
7.2 Intensity distribution 49
7.3 Holographic imaging 50
7.3.1 Algorithm 50
7.3.2 On-axis imaging 55
7.3.3 Off-axis imaging 55
7.3.4 Horizontal parallax only imaging 57
7.4 The effects of using a lens 58
7.5 The effects of a non-parallel illumination beam 59
7.6 Reconstruction 60
7.7 Depth of focus 61
7.8 Speckle 62
7.8.1 Oscillating mirror and laser modulation 64
7.8.2 Homogeneity 66
7.8.3 Transmission factor of the integrator 67

8 Conclusions and recommendations **69**
8.1 Computer Generated Holograms 69
8.2 Speckle 71

A Diffraction **75**
A.1 Single slit diffraction 75
A.2 N-slit diffraction 76

B Algorithm **77**

1

INTRODUCTION

Classical images are always (two-dimensional) images in a flat plane. Whether they are shown on a piece of paper, a television or a computer, it makes no difference. The next step will be to provide the viewer with an extra dimension: depth. The perception of depth relies on depth cues. These cues can be divided into two main groups: physiological depth cues (started to be used) and psychological depth cues (used for a very long time).
The physiological depth cues consists of motion parallax [1]: objects far away move less according to objects close by when the viewer moves his head. Binocular disparity is defined as the difference between the two images as seen by both eyes. Objects nearby jump a bigger distance then objects far away when alternatingly closing the left and right eye. Also accommodation, the ability to focus on objects at different distances, belongs to this group of cues.
The psychological depth cues on the contrary are not the 'real' 3D-depth cues, but more the depth cues created by the viewer's brain. For example occlusion: if one object is before the other so the object behind cannot be seen fully, the brain concludes that the object behind is further away. The same for shading/shadows and size, small objects tend to be pushed to the background by the human brain. This last group of cues is always present in 2D images, like paintings or photographs for example.
In the search to create a 3D display the physiological depth cues are used. Different techniques are known to create 3D images using these cues. Using red and green images the information received with the right eye can be different from the left eye by wearing special glasses with a red and a green filter. The same can be done, even keeping color information, by using polarization to distinguish between the left and right eye, but still glasses are needed.
Going from the above mentioned stereoscopic viewing systems to the so-called auto-stereoscopic viewing systems, the glasses are no longer needed. This group is divided into two subgroups, see also figure 1.1 [2].
The first subgroup contains the volumetric displays. The most important subcategory in this subgroup are the lenticular based displays. A normal LCD display which, by adding a sheet with an array of cylinder lenses (a lenticular), can create an 3D image without viewer worn equipment. For details and more theory behind these lenticular based displays see [3].
The second subgroup is holography. Although a hologram can have different

properties varying from being transmissive to being reflective, here they are divided into optical holograms and computer generated holograms. The optical holograms are made by lighting the wanted (physical) object with a laser. The reflected light, interfering with a reference beam of light, creates an interference pattern which is recorded onto a photographic plate. After developing the photographic plate the object can be re-created by shining the same reference light beam onto the plate. In case of computer generated holography these real objects are not needed anymore. Using a micro-display panel and a virtual representation of the image to be created, the correct interference pattern can be calculated. Building such a set-up and a program to calculate the interference pattern are the main parts of this project.
The aim for this project and this end-report is dual. The first target is to research the possibilities to realize 3D displays based on holography. The second target is to reduce or prevent speckle from developing. This report is therefore divided into two sections. The first section is about holography. The second one is about speckle and how to reduce it. When this project started in November 2004 the main subject was speckle reduction. Due to a change in the research program at Philips Natlab this subject was finalized in favor of a subject change into next-generation 3D displays; Computer Generated Holography.
At the beginning the subject was focussed on speckle and speckle reduction. The goal was to develop a waveguide that could transfer the coherent laser light into incoherent light, homogeneously distributed across the exit-plane of the waveguide. However, in the second part of the research, again speckle returned as a subject of interest. The laser light source used in holography also generates speckle when the image is 'projected' onto a screen.
This report starts with an introduction, this chapter. Chapter 2 is about the basic theory of waves. Properties of waves like superposition and their behavior during interference and diffraction phenomena are described. Chapter 3 is dedicated to the theory of holography. Explaining how holograms can be calculated and what sort of different properties they have. Chapter 4 is used to take a closer look at the micro-displays used to project the hologram. The behavior of light travelling through a birefringent liquid crystal material is discussed. Chapter 5 explains the origin of speckle and presents some statistics of the speckle formed by shining a laser onto a rough surface. Also discussed are methods to reduce speckle. Chapter 6 shows the different set-ups used in the performed experiments. All previous chapters gave the background information for the written program which is able to calculate holograms. In chapter 7 a detailed description of this written program can be found as well as the results of the various experiments. This all leading to chapter 8 wherein the results are being discussed and the conclusions being made.

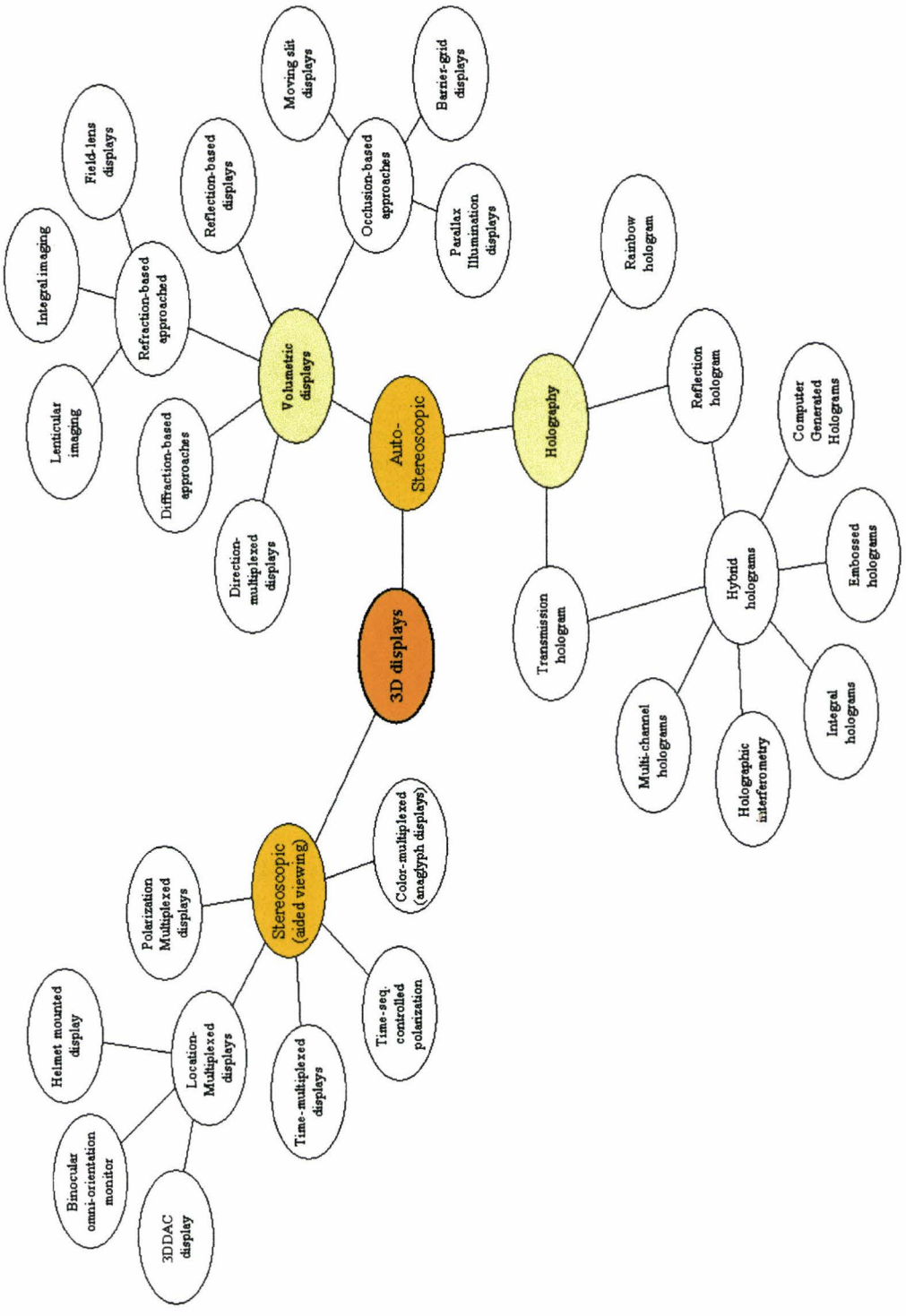

***Fig. 1.1**: An overview of the existing 3D display principles.*

2

PROPERTIES OF WAVES

In this chapter the basic properties of waves are explained. The phenomena that are important, interference and diffraction, are discussed in detail. In short this chapter provides the theory of optics behind the creation of a hologram.

2.1 Waves

A wave can be described by a wave-function $\psi(x,t)$. This function describes the displacement from equilibrium of any part at any time [4]:

$$\psi(x,t) = \psi_0 \exp\left[i(kx - \omega t)\right], \tag{2.1}$$

with ω the angular frequency and k the wave number. To find the transverse velocity v_y at a particular point x, the partial derivative with respect to t has to be taken. The acceleration a_y at a particular point x can be found by taking the partial derivative with respect to t again:

$$a_y(x,t) = \frac{\partial^2\psi(x,t)}{\partial t^2} = -\omega^2\psi_0 \exp\left[i(kx - \omega t)\right] = -\omega^2\psi(x,t). \tag{2.2}$$

In addition to computing the partial derivatives with respect to t it can also be done with respect to x:

$$\frac{\partial^2\psi(x,t)}{\partial x^2} = -k^2\psi_0 \exp\left[i(kx - \omega t)\right] = -k^2\psi(x,t). \tag{2.3}$$

Combining equation 2.2 and 2.3 and using the relation for angular speed $\omega = vk$ [4], the 1D wave equation can be found, at least for undamped homogeneous systems that don't contain sources in the region under consideration [5]:

$$\frac{\partial^2\psi}{\partial x^2} = \frac{1}{v^2}\frac{\partial^2\psi}{\partial t^2}. \tag{2.4}$$

The three-dimensional wave equation can be obtained by generalizing the one-dimensional expression in equation 2.4. In Cartesian coordinates, the position variables x, y and z must certainly appear symmetrically in the three-dimensional equation, for there is no distinguishing characteristics for any of the axes in Cartesian coordinates. The wave $\psi(x,y,z,t)$ is then given by [5]:

$$\frac{\partial^2\psi}{\partial x^2} + \frac{\partial^2\psi}{\partial y^2} + \frac{\partial^2\psi}{\partial z^2} = \frac{1}{v^2}\frac{\partial^2\psi}{\partial t^2}. \tag{2.5}$$

Usually equation 2.5 is written in a more simple from by introducing the Laplacian operator whereupon it becomes:

$$\nabla^2\psi = \frac{1}{v^2}\frac{\partial^2\psi}{\partial t^2}. \tag{2.6}$$

One of the solutions of the wave equation is the plane wave. It consists of waves which form a set of wavefronts, with equal phase, perpendicular to the propagation direction. The mathematical expression for a plane wave that is perpendicular to a given propagation vector $\vec{\mathbf{k}}$ is given by:

$$\psi_p(\vec{\mathbf{r}}, t) = \psi_{0,p} \exp\left[i(\vec{\mathbf{k}} \cdot \vec{\mathbf{r}} \mp \omega t)\right]. \tag{2.7}$$

An idealized point source of light emanates the radiation out radially, uniformly in all directions. The source is said to be isotropic, and the resulting wavefronts are concentric spheres that increase in diameter as they expand out into the surrounding space. The obvious symmetry of the wavefronts suggest that it might be more convenient to describe them in terms of spherical coordinates. In this representation the Laplacian operator is:

$$\nabla^2 \equiv \frac{1}{r^2}\frac{\partial}{\partial r}\left(r^2\frac{\partial}{\partial r}\right) + \frac{1}{r^2\sin\theta}\frac{\partial}{\partial\theta}\left(\sin\theta\frac{\partial}{\partial\theta}\right) + \frac{1}{r^2\sin^2\theta}\frac{\partial^2}{\partial\phi^2}. \tag{2.8}$$

Remember when looking for a description of spherical waves, waves that are spherically symmetrical do not depend on θ and ϕ. The solution of equation 2.6 representing a spherical wave progressing radially outward from the origin, at a constant speed $\vec{\mathbf{v}} = \omega/\vec{\mathbf{k}}$, is the harmonic spherical wave given by:

$$\psi_s(\vec{\mathbf{r}}, t) = \left(\frac{\psi_{0,s}}{|\vec{\mathbf{r}}|}\right) \exp\left[i\vec{\mathbf{k}}(\vec{\mathbf{r}} \mp \vec{\mathbf{v}}t)\right], \tag{2.9}$$

wherein the constant $\psi_{0,s}$ is called the source strength. Notice that the amplitude of any spherical wave is a function of $\vec{\mathbf{r}}$, where the term $|\vec{\mathbf{r}}|^{-1}$ serves as an attenuation factor. This attenuation factor is a direct consequence of energy conservation. So unlike plane waves, spherical waves decrease in amplitude, thereby changing their profile as they expand and move out from the origin.

2.2 Interaction of light waves

A hologram is often described as a three-dimensional picture. A hologram contains information about the size, shape, brightness and contrast of the object being recorded. This information is stored in a very microscopic and complex pattern of interference. The interference pattern is made possible by the properties of coherent, linearly polarized light generated by a laser. In the following sections the physical aspects of light will be discussed.

2.2.1 The principle of superposition

When two or more waves move simultaneously through a region of space, each wave proceeds independently as if the other were not present. The resulting

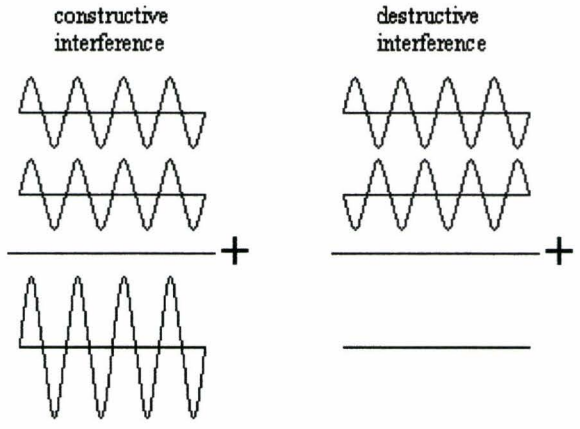

***Fig. 2.1**: Constructive and destructive interference.*

wave 'displacement' at any point and time is the vector sum of the 'displacements' of the individual waves. This is known as the principle of superposition. So, if there are two light waves passing through some common point P, where wave 1 alone causes a displacement Y_1 and wave 2 alone a displacement Y_2, the principle of superposition states that the resultant displacement Y_{res} is given by a vector sum of the two displacements. If both displacements are along the same direction the two can be added algebraically:

$$Y_{res} = Y_1 + Y_2. \tag{2.10}$$

The interference of two sinusoidal waves of the same amplitude and same frequency, travelling in the same direction, can have different solutions. When the two waves are exactly in phase, with their maximum and minimum points matching perfectly, applying the principle of superposition to the two waves result in a wave with the same frequency but twice the amplitude. This is an example of constructive interference, see also figure 2.1. When the two curves are exactly out of phase with the crest of one falling on the trough of the other, the one wave cancels the effect of the other wave. The resultant wave has zero displacement everywhere, an example of destructive interference. Properties of these phenomena will be explored in further paragraphs.

2.2.2 Huygens' wavelets

The wavefront of a propagating wave of light at any instant conforms to the envelope of spherical wavelets emanating from every point on the wavefront at the prior instant, with the understanding that the wavelets have the same speed as the overall wave. An illustration of this principle, known as Huygens' principle, is shown in figure 2.2.
The principle has a shortcoming: it fails to account for the directionality of the wave propagation in time. It doesn't explain why the wavefront at time $t + \Delta t$ is the upper rather than the lower envelope of secondary wavelets.

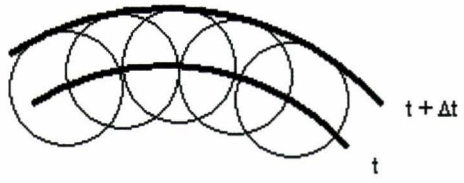

Fig. 2.2: *Huygens' principle; every point is a source of secondary wavelets.*

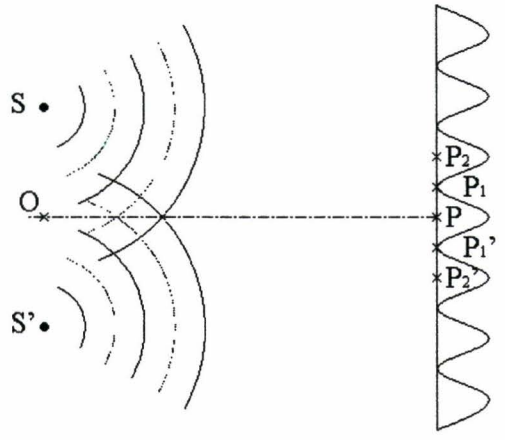

Fig. 2.3: *Two coherent point sources creating an interference pattern.*

This principle will be used to explain the resulting diffraction pattern when light shines through a (single) slit.

2.3 Interference

As already mentioned in paragraph § 2.2.1, constructive interference leads to the maximum amplitude and destructive interference to the minimum. To determine the amplitude at any point the phase difference has to be taken into account. This phase difference results from the path difference d and the initial phase of the point source.
Taking two point sources, S and S' as in figure 2.3, emitting monochromatic waves of the same frequency in a homogeneous medium and with their separation a much greater than the wavelength λ, their wave-equations can be written as [4]:

$$\begin{aligned} \psi_1(t) &= \psi \cos \omega t \\ \psi_2(t) &= \psi \cos(\omega t + \phi). \end{aligned} \tag{2.11}$$

The amplitude ψ_p of the resultant sinusoidal wave at point P is the vector sum of the two individual waves, figure 2.4. The amplitude ψ_p can be found using

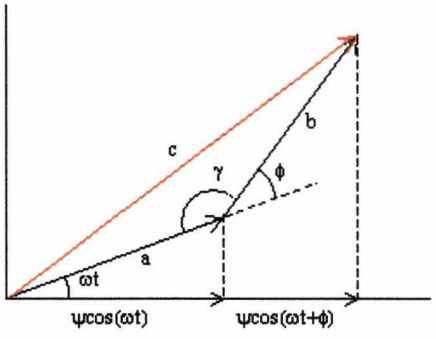

***Fig. 2.4**: Summing two vectors using the cosine rule.*

the cosine rule which states that $c^2 = a^2 + b^2 - 2ab\cos\gamma$:

$$\begin{aligned} \psi_p^2 &= \psi^2 + \psi^2 - 2\psi^2\cos(\pi - \phi) \\ &= \psi^2 + \psi^2 + 2\psi^2\cos\phi \\ &= 4\psi^2\cos^2(\frac{\phi}{2}) \\ \psi_p &= 2\psi|\cos(\frac{\phi}{2})|. \end{aligned} \tag{2.12}$$

Thus the superposition of two sinusoidal waves with the same frequency and amplitude but with a phase difference yields a sinusoidal wave with the same frequency and an amplitude between zero and twice the individual amplitudes, depending on the phase difference.
To obtain the intensity I at point P the average magnitude of the Poynting vector should be taken, S_{avg}. For a sinusoidal wave with amplitude E_p, the intensity can be expressed as [4]:

$$\begin{aligned} I = S_{avg} = \frac{\psi_p^2}{2\mu_0 c} &= \frac{1}{2}\epsilon_0 c\psi_p^2 \\ &= 2\epsilon_0 c\psi^2\cos^2\frac{\phi}{2} \\ &= I_0\cos^2\frac{\phi}{2}. \end{aligned} \tag{2.13}$$

In figure 2.3, along the directions OP, OP_2 and OP_2' crests from S and S' meet (as do troughs), so $\phi = 0$, thereby creating a condition of constructive interference. As a result, light striking the screen at points P, P_2 and P_2' is at maximum intensity I_0 and a bright spot appears.
By contrast, along directions OP_1 and OP_1' crests and troughs meet each other, creating a condition of destructive interference, $\phi = \pi$. So at points P_1 and P_1' on the screen, no light appears, leaving a dark spot.
For interference to occur, the sources need to be coherent and need to have equal polarization, which are stringent requirements. To see the need for coherent

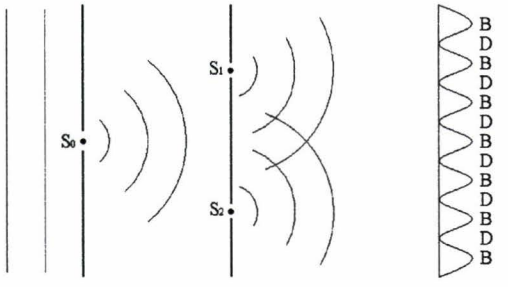

***Fig. 2.5**: The interference pattern resulting from a double slit*

sources more clearly, the following example is given: suppose for a moment that sources S and S' are in fact two corks bobbling up and down on a quiet pond. As long as the two corks maintain a fixed relationship between their vertical motions, each will produce a series of related crests and troughs, and observable interference patterns in the overlap region will occur. But if the two corks bob up and down in a random, disorganized manner, no series of related, fixed-phase crests and troughs will form and no interference patterns of sufficiently long duration can develop, and so interference will not be observed. Regarding the necessity for the interfering waves to have equal states of polarization, there are three conditions of Fresnel and Arago which state [5]:

1. Two orthogonal, coherent polarization states cannot interfere in the sense that no fringes result.

2. Two parallel, coherent polarization states will interfere in the same way as will natural light.

3. The two constituent orthogonal polarization states of natural light cannot interfere to form a readily observable fringe pattern. This last point is understandable, since these polarization states are incoherent.

2.3.1 Young's double slit interference experiment

Consider a hypothetical monochromatic plane wave illuminating a long narrow slit. From that primary slit, light will be diffracted out at all angles in the forward direction and a cylindrical wave will emerge. Suppose that this wave falls on two parallel infinitesimally wide slits, S_1 and S_2, as in figure 2.5. Cylindrical waves radiating out from the two secondary sources maintain a fixed phase relationship with each other as they spread out and overlap on the screen. They produce series of alternate bright and dark regions, referred to as interference fringes.
With the help of the principle of superposition the intensity profile can be calculated. Doing this the following conditions have to be taken care of: light from the slits S_1 and S_2 has to be coherent and of the same wavelength.
In figure 2.6 light waves from S_1 and S_2 spread out and overlap at an arbitrary point P on the screen. The phase difference between the two waves arriving at

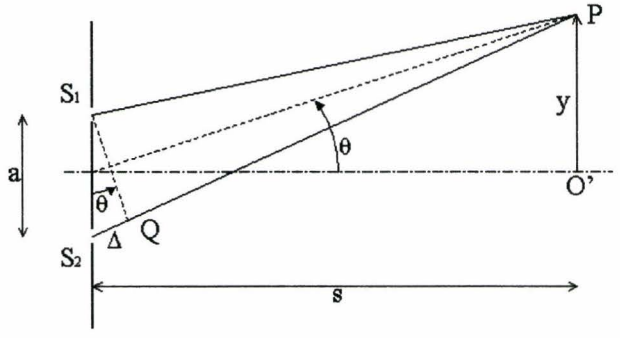

***Fig. 2.6**: The parameters used in calculating the interference pattern*

point P determines what happens there. This phase difference can be expressed in terms of a path difference Δ related to the wavelength [5]:

$$\Delta = S_2P - S_1P = a\sin\theta, \tag{2.14}$$

for the distances S_1P and QP are equal and $\sin\theta = \frac{\Delta}{a}$ in triangle S_1S_2Q.
If the path difference is equal to λ or some multiple of λ, the two waves arriving at P result in constructive interference. If on the other hand, if the path difference at P is an odd multiple of $\frac{\lambda}{2}$, they will destructively interfere. The conditions for a bright fringe to appear are dependent on the distance a between the slits and the wavelength λ of the light:

$$\Delta_{bright} = a\sin\theta = m\lambda. \tag{2.15}$$

The number m is called the order number counted from the central fringe. Because θ is small, $\sin\theta$ can be replaced by $\tan\theta = \frac{y}{s}$. Then from equation 2.15 the y-position of the bright fringes can be determined:

$$y_m \simeq \frac{m\lambda s}{a}, \tag{2.16}$$

with m again the order number. The phase difference between the rays coming from the two separate slits is:

$$\phi = k(r_1 - r_2) = k\Delta = \frac{2\pi a}{\lambda}\sin\theta \simeq \frac{2\pi a}{\lambda}\tan\theta \simeq \frac{2\pi a y}{\lambda s}. \tag{2.17}$$

Recalling equation 2.13, the intensity can be rewritten as:

$$I = I_0\cos^2\left(\frac{ya\pi}{\lambda s}\right). \tag{2.18}$$

Remember that we assumed that each slit was infinitesimally wide, and so the cosine-squared fringes are an idealization. The actual amplitude of the pattern drops off with distance on either side of the central fringe. This effect originates from the equal distribution of energy within the wavefront. At large distances the wavefront of the cylindrical shaped wave has become large so the energy of the wave at a particular point will be less.

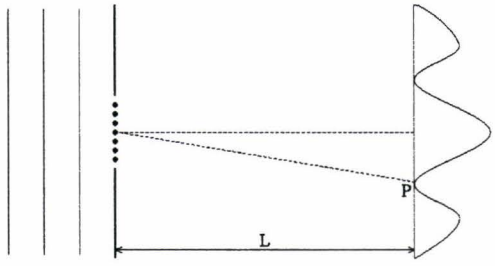

***Fig. 2.7**: A diffraction pattern from a single slit opening.*

2.4 Diffraction

The ability of light to bend around corners, a consequence of the wave nature of light, is fundamental for both interference and diffraction. Diffraction is simply any deviation from geometrical optics resulting from the obstruction of a wave front of light by some obstacle or some opening. This occurs when light waves pass through small openings, around obstacles, or by sharp edges. If both the source and the screen are relatively close to the obstacle forming the diffraction pattern, it is described as near-field diffraction or Fresnel diffraction. If the source, obstacle and screen are far enough away that the waves from the source to the obstacle can be considered parallel, the phenomenon is called far-field diffraction or Fraunhofer diffraction. Within the field of interest of holography the distances are relatively large, in the region of Fraunhofer diffraction.

2.4.1 Single slit

The overall geometry for diffraction by a single slit is shown in figure 2.7. The slit opening, seen in cross section, is in fact a long, narrow slit, perpendicular to the page. The pattern shown along the screen gives a rough idea of intensity variation in the pattern. A wide central bright fringe is observed, bordered by narrower regions of dark and bright. To determine the location of the minima and maxima on the screen, the slit opening through which a plane wave is passing is divided into many point sources (Huygens' sources), as shown by the series of tiny dots in the slit opening in figure 2.7. These numerous point sources send out Huygens' spherical waves, all in phase, towards the screen. There, at a point such as P, light waves from the various Huygens' sources overlap and interfere, forming the variation in light intensity [5], for more details see appendix A.

$$I(\theta) = I(0)\left(\frac{\sin\beta}{\beta}\right)^2 \qquad (2.19)$$
$$\beta = \frac{\pi a}{\lambda}\sin\theta \quad ,$$

with θ the angle of the path according to the normal of the slit and a the width of the slit. Thus, diffraction considers the contribution from every part of the wave front passing through the aperture. Interference by contrast considers each slit as a point source instead of multiple sources within one slit, ignoring

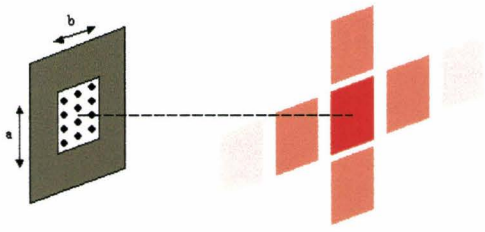

***Fig. 2.8**: A rectangular aperture with the resulting diffraction pattern.*

details of the wave fronts caused by passing through a slit opening. Equation 2.19 locates the minima y_{min} due to diffraction on the screen in terms of the slit width a, slit-to-screen distance L, wavelength λ and order m:

$$y_{min} = \frac{m\lambda L}{a}, m = 0, \pm 1, \pm 2, \ldots. \tag{2.20}$$

2.4.2 Rectangular aperture

The limited case of a single slit is a rectangular aperture as shown in figure 2.8. Again using Huygens' principle the area within the aperture may be seen as being covered with coherent secondary point sources. The strength of these sources are assumed to be constant over the entire area. The intensity at a certain distance R is [5]:

$$\begin{aligned} I(x,y) &= I_0 \left(\frac{\sin\alpha'}{\alpha'}\right)^2 \left(\frac{\sin\beta'}{\beta'}\right)^2 \\ \alpha' &\equiv \frac{kax}{2R} \\ \beta' &\equiv \frac{kby}{2R}. \end{aligned} \tag{2.21}$$

Along the β'-axis, $\alpha' = 0$, and the subsidiary maxima are located approximately halfway between zeros, that is, at $\beta'_m = \pm\frac{3\pi}{2}, \pm\frac{5\pi}{2}, \pm\frac{7\pi}{2}, \ldots$. The relative irradiances are approximated by:

$$\frac{I}{I_0} = \frac{1}{\beta'^2_m}. \tag{2.22}$$

This goes similarly along the α'-axis. The intensity drops off rather rapidly from 1 to $\frac{1}{22}$ to $\frac{1}{62}$ and so on. So the first order had an intensity 22 times lower than the zeroth order.

2.5 Gratings

If an aperture is prepared with thousands of adjacent slits, this is a so-called transmission diffraction grating. The width of a single slit, the opening, is given by a, and the distance between slit centers is given by d, see figure 2.9. Note that the spreading of light occurs always in a direction perpendicular to the

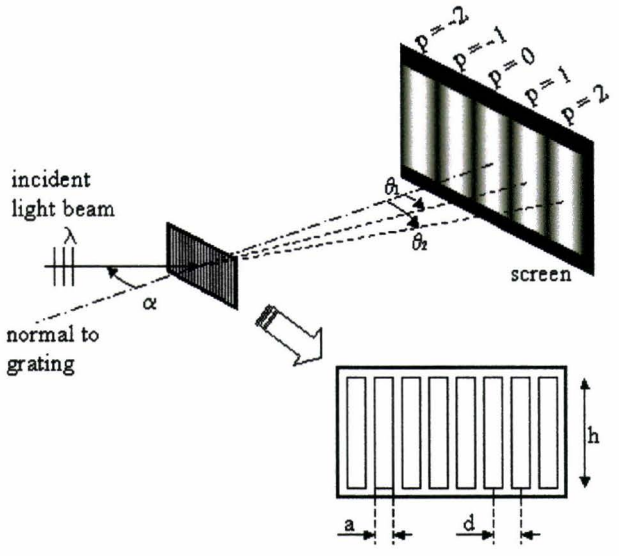

***Fig. 2.9**: The diffraction pattern coming from a grating.*

direction of the long edge of the slit opening, that is, since the long edge of the slit opening is vertical in figure 2.9, the spreading is in the horizontal direction, along the screen. The resulting diffraction pattern is a series of sharply defined, widely spaced fringes. The central fringe, on the symmetry axis, is called the zeroth order fringe. The successive fringes on either side are called first order, second order, etcetera. They are numbered according to their position relative to the central fringe, as denoted by the letter p. The intensity pattern on the screen is a superposition of the diffraction effects from each slit as well as the interference effects of the light from all the adjacent slits. The combined effect is to cause overall cancellation of light over most of the screen with marked enhancement over only limited regions. The location of the bright fringes is given by the following expression called the grating equation:

$$d(\sin\alpha + \sin\theta_p) = p\lambda, \tag{2.23}$$

where d the distance between the slit centers, α the angle of incidence of light measured with respect to the normal to the grating surface, θ_p the angle locating the p-th order fringe, p an integer taking on values of $0, \pm 1, \pm 2$, etcetera and λ the wavelength of the light. The intensity of the fringe pattern for N slits is given by the interference intensity expression:

$$I = I_0 \frac{\sin^2(N\gamma)}{\sin^2(\gamma)}, \tag{2.24}$$

with $\gamma = \frac{\pi d}{\lambda}\sin\theta$. If the interference term is modulated by the single slit diffraction envelope, equation 2.19 the total intensity profile will be:

$$I = I_0 \frac{\sin^2(\frac{\pi a}{\lambda}\sin\theta)\sin^2 N(\frac{\pi d}{\lambda}\sin\theta)}{(\frac{\pi a}{\lambda}\sin\theta)^2 \sin^2(\frac{\pi d}{\lambda}\sin\theta)}. \tag{2.25}$$

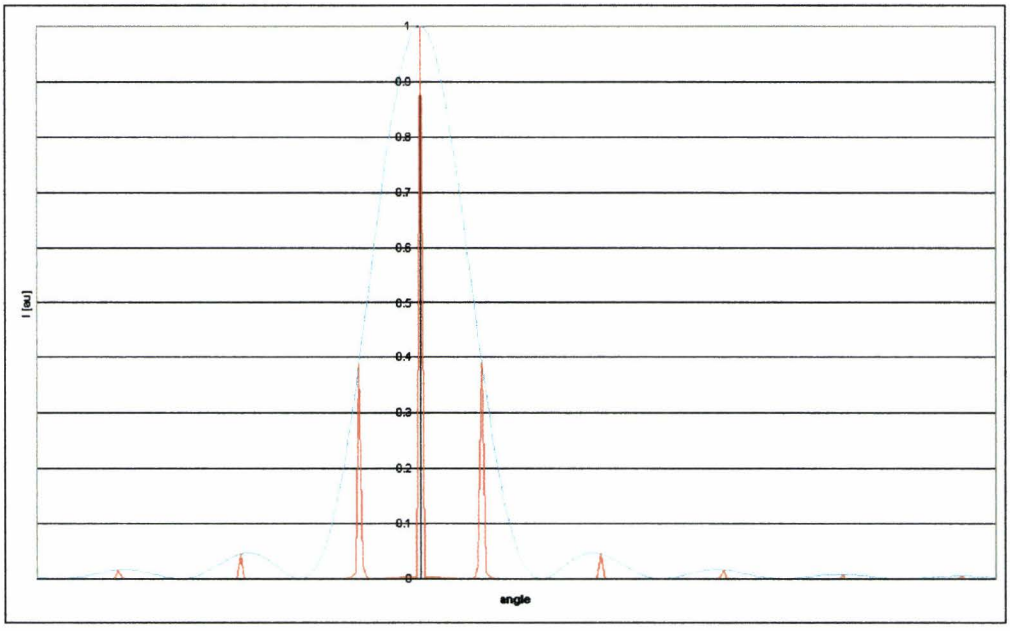

***Fig. 2.10**: The intensity pattern for an ideal grating with $d = 2a$. The blue line represents the intensity profile due to diffraction only and the red line the total intensity profile due to diffraction and interference.*

In the ideal situation, based on equation 2.25, a grating with $d = 2a$ leads to an intensity distribution as shown by the red line in figure 2.10. The light-blue line represents the effect on the intensity due to diffraction. As indicated in §2.4.2 the first order has an intensity which is 22 times lower than the zeroth order.

3

HOLOGRAPHY

Holography originated from a British/Hungarian scientist D. Gabor, when he tried to improve the resolution of his electron microscope in 1947. Using a mercury arc lamp, the non-coherent light source resulted in distortions in his images. He derived the term hologram for these images, coming from the Greek words 'holos', meaning "whole" and 'gramma' meaning "message". He realized that his images contained more information than a normal photograph. He tried to make his light source coherent by sending it through a pinhole, but the quality of his first holograms were poor.
Lacking a proper coherent light source, the interest for holography faded until the invention of the laser at the Bell Laboratories in 1958. A new era erupted and the coming years were the years of holography. Further improvement of the laser and the film technology has made the technique available for everyone.

3.1 Object and reference waves

In holography the wavefronts are being reconstructed, not the intensity distribution like in photography. These wavefronts contain all the optical information contained in the original light waves. The key notion of holography is to record the result of interference between the object beam ψ_{obj} and a coherent reference beam ψ_{ref} [6]. In optical holography this can be done by reflecting some of the original light from the laser source directly to the recording plane in stead of first going to the object's surface. Then afterwards let them interfere at the recording plane. In Computer Generated Holography (CGH) these two laser beams, the one reflecting from the object and the other one as a reference beam, can be separated. The reference beam can be seen as a light source at infinity so plane waves will hit the recording plane. In the complex notation this wave is written as:

$$\psi_{ref}(z) = \psi_0 \exp[i(kz + \phi)]. \tag{3.1}$$

An object point is represented by a point source where a spherical wave starts towards the recording plane, which is given by:

$$\psi_{obj}(r) = \frac{\psi_0}{r} \exp[i(kr + \phi)]. \tag{3.2}$$

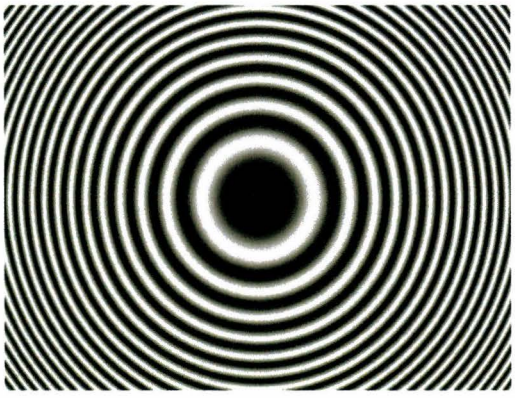

***Fig. 3.1**: A Fresnel Zone Plate used to focus a coherent laser beam into a point.*

When constructing a hologram, the resultant wave amplitude, using the principle of superposition, at each point at a holographic plane is given by [7]:

$$\psi_{tot} = \psi_{obj} + \psi_{ref}. \tag{3.3}$$

Omitting the constant factor $(2\mu_0 c)^{-1}$ in equation 2.13, the intensity can be expressed as the square of the wave amplitude [8]:

$$I_{tot} = |\psi_{tot}|^2 = |\psi_{obj}|^2 + |\psi_{ref}|^2 + 2\Re\{\psi^*_{ref}\psi_{obj}\}. \tag{3.4}$$

The first two terms arise from object self-interference and reference wave bias, respectively, and manifest either unwanted artifacts or low modulation in the output image. The real-valued last term comprises the information necessary to reconstruct the desired image; this term fully describes the interference between the spherical emitters and the reference wave.

3.2 Fresnel Zone Plate

Using lenses a parallel beam of light can be focussed into one point. Using coherent light this can also be done with a Fresnel Zone Plate, like in figure 3.1. If the incident light consists of plane wavefronts then a special amplitude modulation hologram is needed to get constructive interference at a fixed point P. This hologram will consist of zones and the zone radii required to make the zones half-period zones relative to a fixed point P are [9]:

$$R_N^2 = \left(r_0 + \frac{N\lambda}{2}\right)^2 - r_0^2 = r_0^2\left[N\left(\frac{\lambda}{r_0}\right) + \frac{N^2}{4}\left(\frac{\lambda}{r_0}\right)^2\right], \tag{3.5}$$

with R_N the radius of the N-th zone, and r_0 the distance of the focal point. If $\lambda/r_0 \ll 1$ the remaining part of equation 3.5 becomes:

$$R_N^2 = \sqrt{Nr_0\lambda}. \tag{3.6}$$

The radii of the successive zones increase proportional to $\sqrt{N}$.

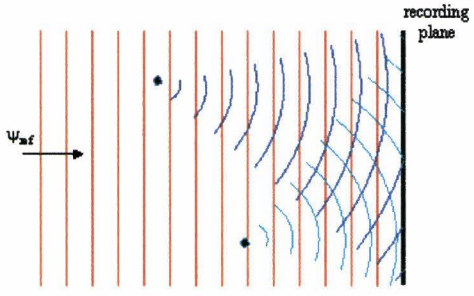

***Fig. 3.2**: Using multiple points to build an object, with each generating a spherical wave towards the recording plane.*

A Fresnel Zone Plate can be an amplitude plate as well as a phase plate. The phase at the focal point of this Fresnel Zone Plate should be exactly in phase so the light constructively sums to a single point of light. This can be reversed: in stead of shining the Fresnel Zone Plate with a plane wave forming a point, a point source interfered with a plane wave results in a Fresnel Zone Plate. Although the Fresnel Zone Plate consists of very small fringes especially at large radii, the zone plate can still be made on a panel with (large) pixels. The space between the fringes is dependent on the distance of the focal point of the Fresnel Zone Plate. Independent of the size of the pixels a sharp point can be generated, only the distance of that point to the panel is affected by the size of the pixels.
The amplitude of the wave depends on the amount of rings within the Fresnel Zone Plate. When it has N rings the amplitude at the focal point will be N-times the amplitude compared to a wholy unobstructed wavefront. The irradiance therefore will be N^2 times as great.

3.3 Point source summation

An object can be built from a multitude of points. When summing their individual contributions to the amplitude and phase in recording plane, they form a recording of the complete object. Thus the object beam is constructed out of multiple spherical waves who's contributions are being superimposed at each point in the recording plane, see also figure 3.2. The reference wave is again represented by equation 3.1. The object wave, constructed out of the many point source waves represented by equation 3.2, can be obtained by summing all the point sources present. Adding these waves together leads to the intensity $I(x, y, z)$ at the recording plane:

$$\begin{aligned} I(x,y,z) &= 2\Re\left[\psi^*_{ref}\psi_{obj}\right] \\ &= 2\Re\left[\psi_{0,ref}\exp[-i(kz+\phi)]\sum_n \frac{\psi_{0,n}}{r_n}\exp[i(kr_n+\phi_n)]\right] \quad (3.7) \\ \text{with} \quad |r_n| &= \sqrt{(x-x_n)^2+(y-y_n)^2+(z-z_n)^2}. \end{aligned}$$

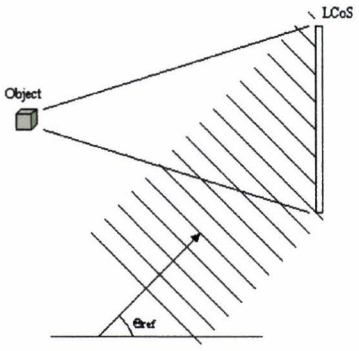

***Fig. 3.3**: Using off-axis holography the reference beam falls not perpendicularly onto the panel, but at a certain angle.*

Whereas $I(x, y, z)$ represents the intensity amplitude at a point in the hologram plane at z_h and $\psi_{0,i}$ is the amplitude of a point from the object. The z'-axis is normal to the center of the recording plane and extends through the center of the reconstructed 3-D scene volume. The wave number of the light is given by k, which is dependent on the wavelength of the light used.

3.4 Phase versus amplitude hologram

A hologram may be an absorption type which produces a change in the amplitude of the reconstruction beam or a phase type hologram which produces phase changes in the reconstruction beam due to a variation in the refractive index or thickness of the medium (or both). Phase holograms have the advantage over amplitude holograms to have no energy dissipation within the hologram medium. Holograms recorded in photographic emulsions change both the amplitude and the phase of the illuminating wave. The shape of the recorded fringes depends on the relative phase of the interfering beams.

3.5 Off-axis holograms

In case of off-axis holography the reference beam doesn't fall onto the panel perpendicularly, but at an certain angle [10]. The advantage of a reference beam at an angle is that it is decoupled from the object beam. This situation is shown in figure 3.3. For the phase of the light waves coming from the object equation 3.2 still counts. But the phase of the light waves coming from the reference source cannot be taken uniform and constant. For each pixel on the panel the phase of the reference beam will be:

$$\phi_{ref} = \phi_0 + \frac{2\pi x p}{\lambda} \sin\theta_{ref}. \tag{3.8}$$

The intensity is then given by equation 3.7 resulting in a multiplication between the summation of all the waves coming from the points and the reference wave.

$$I = \sum \cos\left(\frac{2\pi r}{\lambda} + \phi\right) \cos\left(\phi_0 + \frac{2\pi x_h p}{\lambda} \sin\theta_{ref}\right). \tag{3.9}$$

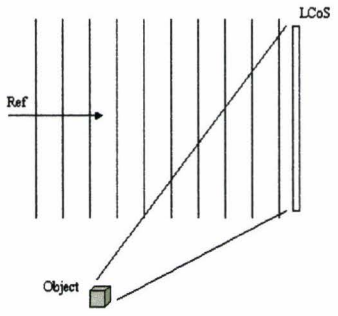

***Fig. 3.4**: Creating an image at a larger angle (according to the normal) then the perpendicular projection of the screen.*

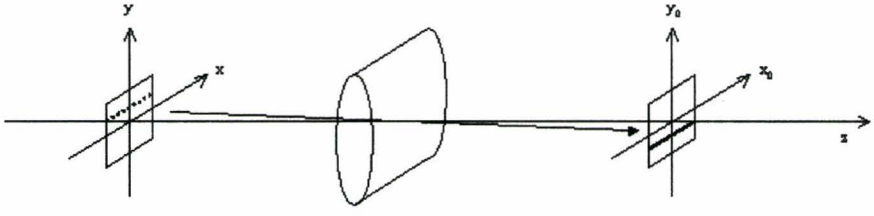

***Fig. 3.5**: Using a cylindrical lens a normal projection is created in the vertical direction and an interference pattern in the horizontal direction.*

A second possibility is to create an image out of the perpendicular plane with a perpendicular reference beam, see figure 3.4.

3.6 Horizontal parallax only

Horizontal parallax only (HPO) is a sort of hybrid between the normal projection method (using a lens) and the holographical method. In stead of a spherical lens a cylindrical lens is used to produce an HPO, see figure 3.5. This cylindrical lens creates a normal image in vertical direction but allows a holographic image in horizontal direction. So a row of pixels is transferred directly to the screen, but the pixels within the row are allowed to contain holographic information to create an interference pattern.

4

DISPLAYS

In our set-up for generating computer generated holograms, LCoS micro-display panels are used to image the holograms on. Because holograms are influenced by the polarization, amplitude and phase, the properties of the LC material within the panels are viewed in closer perspective. For LC material is capable of changing these three properties of light.

4.1 Liquid crystal

Liquid crystals (LCs in general) have long cigar-shaped molecules that can move about, and consequently, like ordinary liquids, they lack positional order [5]. Nonetheless, like crystals, their molecules strongly interact to sustain a large-scale orientational order. There are three types of liquid crystals distinguished by the ways in which their molecules align. One of them is the nematic variety in which the molecules tend to be more or less parallel, even though their positions are fairly random.

To prepare a parallel nematic cell, first one face of each of two pieces of flat glass has to be coated with a transparent electrically conducting metallic film, such as indium tin oxide. These two windows will serve as the electrodes, between which the LC material is placed and across which a controlling voltage can be applied. The LC molecules in contact with the windows would like to be oriented in a direction that is both parallel to the glass and to each other. To accomplish that, it is necessary to create a template of parallel ridges along which the LC molecules can align. The simplest way of doing that is to carefully rub the indium tin oxide surface, thereby producing parallel microgrooves.

When the thin space (up to about $10\mu m$) between two such prepared glass windows is filled with nematic LC, the molecules in contact with the microgrooves anchor themselves parallel to the ridges. The LC molecules essentially drag each other into alignment, and soon the entire liquid is similarly oriented, see figure 4.1. The direction in which the molecules of a liquid crystal are aligned is known as the director.

Because of their elongated shape and ordered orientation the liquid crystal molecules behave en masse as an anisotropic dielectric, one that's positive uniaxial birefringent. The long axis of the molecules defines the direction of the extraordinary index or slow axis. A ray of light linearly polarized parallel to

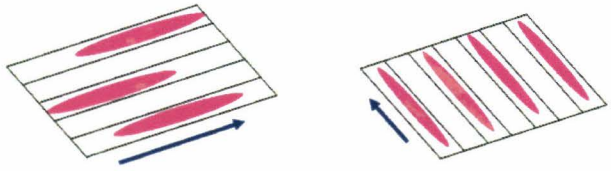

***Fig. 4.1**: The orientation of the LC molecules according to the microgrooves on the glass.*

the LC director will be an extraordinary ray and will experience an ongoing phase change as it traverses the cell. By contrast, a ray linearly polarized at 45° to the director will suffer a retardance $\Delta\phi$ just as if it has passed through a birefringent crystal.

4.1.1 The liquid crystal variable retarder

Suppose a voltage (V) is applied across the cell, thereby creating an electric field perpendicular to the glass windows. Electric dipoles are either present or induced, and the LC molecules experience torques that cause them to try to rotate into alignment with the field. As the voltage increases the molecules (except for those anchored to the inner surfaces of the windows), more and more turn towards the direction of the field, decreasing the birefringence, $\Delta n = (n_e - n_o)$, and the retardance $\Delta\phi$ as well. The birefringence is a function of the voltage, temperature and wavelength, see also figure 4.2:

$$\Delta\phi(V, T, \lambda_0) = \frac{2\pi}{\lambda_0} d\Delta n(V, T, \lambda_0). \tag{4.1}$$

Maximum retardance (typically $\approx \frac{\lambda_0}{2}$) is obtained when the applied voltage is zero. The retardance when V is large is at a minimum of around zero, when a compensator is used to cancel the residual retardance of the anchored layers. When the incident light is polarized parallel to the slow axis, the device can be used as a voltage-controlled phase modulator. It can change the phase delay the light will experience in traversing the cell. Alternatively, when the light has components parallel and perpendicular to the slow axis, the LC cell functions as a continuously variable retarder over a broad range of wavelengths. By placing the cell between crossed polarizers, it becomes a voltage-controlled light modulator.

4.1.2 The liquid crystal display

Imagine that one of the windows of the parallel LC cell is now rotated 90° in its own plane. This drags around the nematic liquid so that its molecular layers spiral a quarter of a turn about the twist axis normal to the windows. The result is a so-called twisted nematic cell. The molecules are aligned vertically on one window, and gradually they are rotated, layer upon layer, until they are horizontal on the other window.

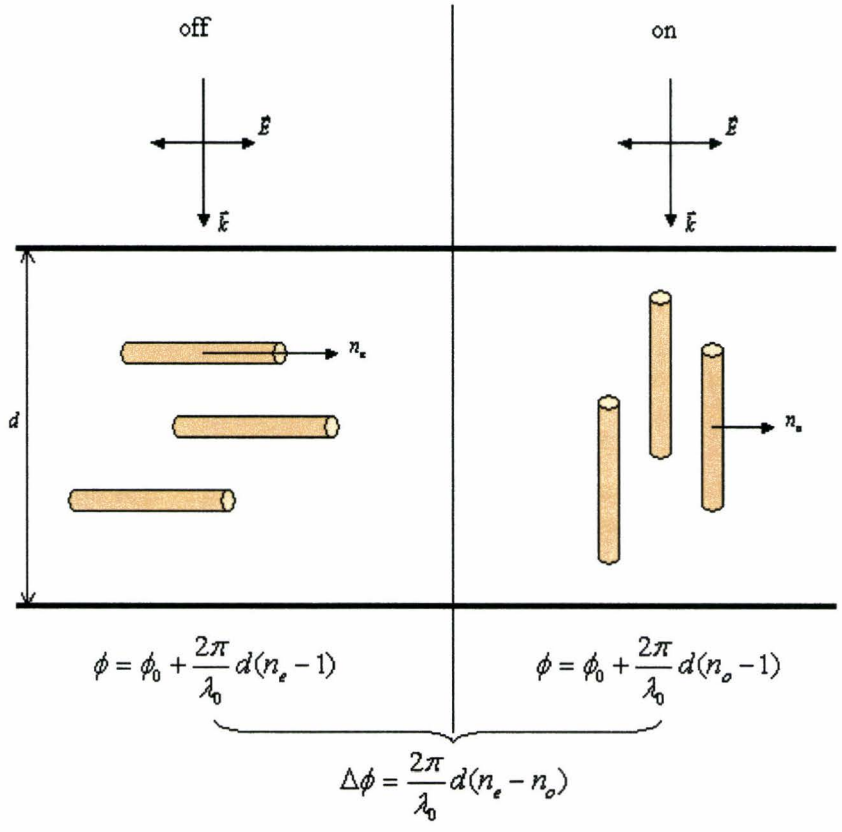

Fig. 4.2: *The phase difference due to the alignment of the LC molecules.*

Upon putting a voltage across the cell, an electric field parallel to the twist axis is set up throughout the liquid crystal. Consequently, the LC molecules (except for those anchored to the windows) turn into alignment with the field. The twisted structure of the cell vanishes, and it loses its stability to rotate the plane of polarization of incident light. When the E-field is removed, the cell reverts back to its twisted configuration and can again rotate light. If the cell is now placed between crossed linear polarizers, it becomes a voltage controlled switch that can transmit or absorb an incident beam of light.

The simplest liquid crystal display (LCD) is illuminated by ambient light. Therein lies its principal virtue: it consumes very little electrical power because it isn't self-luminous.

To make an LCD, two polarizers are put around the LC cel, see figure 4.3. Light enters from above and is immediately linearly polarized in one direction by the first polarizer. With no voltage applied on the electrodes the light emerges from the twisted LC cell, oscillating perpendicular to the entrance direction. Then it passes through the second polarizer, unaffected by it.

When a voltage is applied across the cell, the liquid crystals reorients themselves and lose their ability to rotate the plane of polarization unlike the twisted orientation of the LC molecules without any applied voltage. One direction

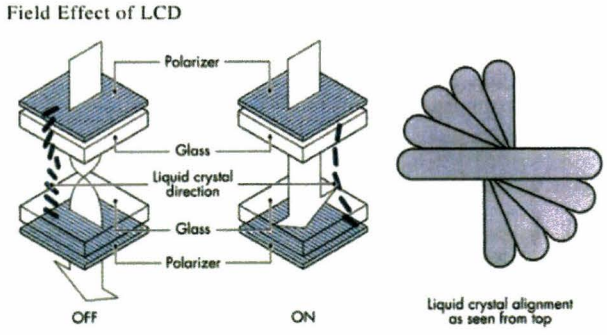

***Fig. 4.3**: Light throughput through an LCD panel, with or without a voltage applied on the electrodes.*

polarized light enters and leaves the cell, only to be completely absorbed by the second polarizer; the exiting window is now black, and no light emerges.

4.1.3 Liquid crystal on silicon

Liquid crystal on silicon (LCoS) is a new technology related to LCD but which works differently. The liquid crystal material has a twisted nematic structure like other LCDs, but the liquid crystal material is coated directly over the surface of a silicon CMOS chip. The chip contains the control circuitry and is coated with a reflective surface (mostly aluminum). Spacers are used either on the outside or distributed around the chip to maintain the cell gap uniformity. This space can be as small as $1\mu m$. The alignment layer is there to ensure that the crystals are all in the same direction. As it is necessary to apply an electric field to the liquid crystal a second transparent electrode above the crystals is added. Using these, several million pixels can fit in an area as small as one square inch.
The LCoS micro-displays used, use a twisted nematic liquid crystal [11]. When an electric field is applied to the crystal the amount of twist varies. Using this principle a beam of light is passed through a polarizer (externally) to make the light waves travel in a single direction. The twisted nematic liquid crystal causes direction of the polarized light to change. This light is then reflected off the LCoS reflective coating and travels through the liquid crystal layer for a second time providing it is in the correct direction after leaving the LCoS material it then passes through a second polarizer (also externally).
Color is created in a variety of ways [12] [13] [8]. The simplest is to include three LCoS panels, one each for red, green and blue light elements. Generating three different images and combine them to make a full-colored image. Alternatives include color pixelisation, field sequential color (FSC) and a scrolling color wheel, which enables just one panel to be used.
The properties of LCoS panels are summarized by mentioning the abilities of the LC material inside the panels. This LC material acts as a phase modulator, an amplitude modulator and both at the same time.

5

SPECKLE

For projection purposes a low-energy consuming projector is wanted which creates a bright, homogeneous image. To enable down-scaling the size of a normal projector to that useful for the mobile market, the light source is changed to three or more Light Emitting Diodes (LEDs). But recent expectations for LEDs based projection are that the red source will lag behind insufficient in source brightness and lumen output, compared to the other two primary colors, green and blue. This means that the red LED will be limiting the amount of light output. Replacing the red LED by a semiconductor laser could offer a solution to increase the lumen output of a projector.

One of the main problems of using a laser is the occurrence of speckle. Speckle appears when coherent light is scattered by a rough surface. When an observer is looking at a laser-illuminated screen, the scattered laser light will produce an interference pattern in his/her eye. The pattern depends on the properties of the screen (for example roughness) and the optical properties of the human eye. The observer will notice, superposed on a homogeneous image, a more or less random pattern of bright and dark regions, which will change when the position of the eye is changing. The spots will get smaller if the observer is moving towards the screen and the other way around by moving away. A lateral movement of the eye will end up in a movement of the speckle pattern. The direction and the velocity of the movement of the pattern depends on whether the viewer is near- of far-sighted. This effect makes an unperturbed vision of a laser-projected image impossible.

In a previous study [14] a number of ways have been described how to reduce the speckle by reducing the coherence length of the laser beam. The most promising method seemed to be based on a rod integrator. This is a bar of glass containing mirrors at both ends. The entrance plane consists of a nearly fully reflective mirror (98%) with a small pinhole, whereas the exiting plane consists of a partly transparent mirror.

Another way of shortening the coherence is to modulate the laser it self. Applying very short pulses, more modes are able to maintain within the laser resulting in a reduction of the coherence length of the emitted laser beam.

Placing an oscillating mirror in the optical pathway can be used to change the angle of the laser beam hitting the lenses, thereby changing the speckle pattern versus time. The frequency of the mirror oscillation must be fast enough so that

the mirror oscillates several times within the integration time of the camera or the human eye.
Another problem associated with laser projection is the illumination homogeneity of the generated image. Projecting a divergent laser beam onto a screen gives a round, Gaussian-shaped intensity distribution. Redistributing the light by using the rod integrator leads to a rectangular, more homogeneous shaped profile.
When battery fed, the power consumption of the mobile projector needs to be as low as possible, therefore light losses in the system have to be minimized. For optimizing purposes it has to be known how much of the light is wasted in the different optical components, therefore the transmission will be measured.
In the next part the laser diode will be described for that is the light source used. One of the properties of the laser will be used to lower the speckle formation. This speckle formation and some statistics are discussed in §5.2. After that several speckle reduction methods are introduced in the last paragraph.

5.1 Laser diode

The laser diodes are a special class of lasers [5]. They differ from conventional lasers in two points:

- For the classical lasers the laser-active atoms (molecules or ions) are independent of one another and only the same energy levels are used for the laser process. This means in principle that in order to produce a population inversion an infinite number of atoms can contribute (Boltzmann statistics).

- This is not the case with semiconductor lasers. Here a defined energy level can only be occupied by two active particles (electrons, Pauli principle). In semiconductors, the wave functions of the individual atoms overlap to form a common energy band and the extent to which the level is occupied follows the Fermi Dirac statistics. When considering the laser process, the transition between the distribution of population in two energy bands instead of two energy levels must be taken into account as for conventional lasers.

Laser diodes don't have any specifically defined emission wavelength, because there are no two discrete energy levels that are responsible for the laser process as with traditional lasers, but rather an energy distribution of electrons in energy bands. The second important difference concerns the lateral propagation of the laser light within the semiconductor layers; the spatial intensity distribution of the laser beam is defined by the laser medium and not by the resonator as for normal lasers.
Figure 5.1 shows the situation of a population inversion in a semiconductor. By doping the basic semiconductor material band structures can be created with different properties. A very simple example may be the semiconductor diode where the basic material, germanium or silicon, is converted into p or n conducting material using suitable donators and acceptors. By the connection

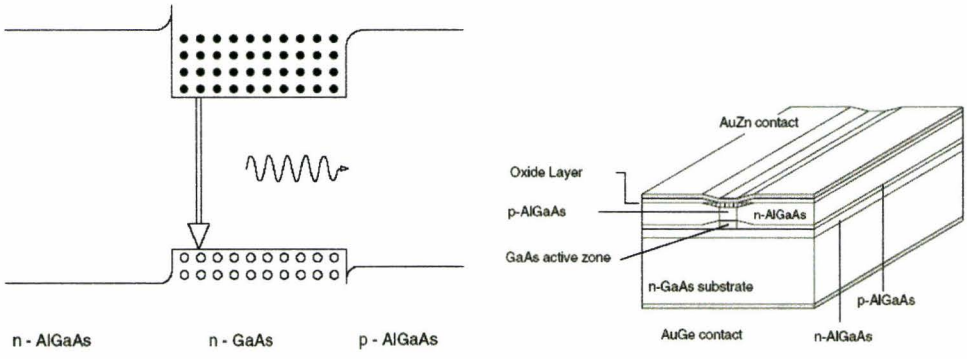

***Fig. 5.1**: Left: Energy band diagram of a N n P structure. Right: Buried structure. The active zone had been buried between some layers which ensure an optimal beam guidance in the zone.*

of the doted materials a barrier (also called active zone) is formed. It will be responsible for the properties of the element. In this concept a layer GaAlAs is brought on the layer of GaAs. The slightly higher band gap of GaAlAs compared to GaAs ensures that a potential barrier is created between both materials in a way that charge carriers accumulate here and the population inversion is formed, figure 5.1.

5.1.1 Light versus current

Above a characteristic threshold current I_s at which the laser diode starts lasing, the ideal laser diode shows a linear dependence between optical output power and laser current, figure 5.2 [2]. Then the higher the injection current, the more light output is reached. And also the output is more single-mode. Below the threshold, the optical amplification is not sufficient. The light is emitted spontaneously, such as for an LED.
The coherence length L_{coh} of laser diodes can be calculated from the spectral width $\delta\lambda$ of each emitted spectral line respectively from the FWHM of the spectrum:

$$L_{coh} = \frac{\lambda^2}{\delta\lambda}. \tag{5.1}$$

Knowing that the larger the current the more single mode the laser will become (the smaller $\delta\lambda$), this will result in the coherence length becoming longer. Due to a smaller spectral width, for the laser becomes more single mode at higher injection current, the coherence length elongates. A typical semiconductor with a wavelength of 638 nm at maximum power has a spectral line width of 1 nm and a coherence length of about 0.4 mm.
With the dominance of stimulated emission that results from a population inversion [6], the only remaining requirement for laser action is to confine emission so that it is directed primarily along the junction boundaries and undergoes amplification or gain before being emitted from the semiconductor material. In some diode laser devices, confinement of emitted light to the optical cavity

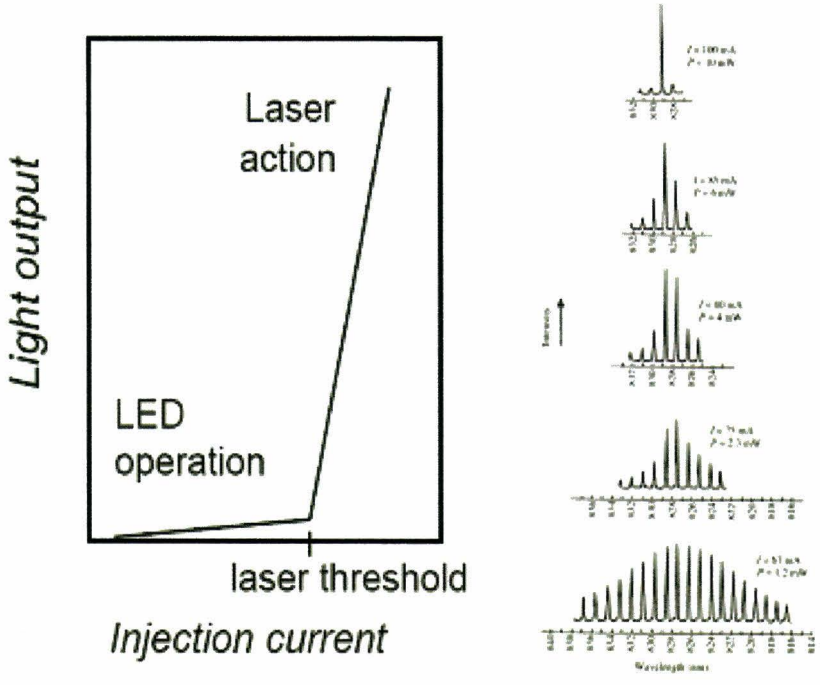

***Fig. 5.2**: Typical current versus light output graph. The higher the current the fewer modes survive.*

is often achieved by applying reflective coatings to opposite ends of the laser crystal. However, in most cases, even this step is not required. Because the refractive index of most semiconductor materials is significantly higher than that of air, sufficient internal reflection occurs at the boundaries of the crystal to confine the emission and sustain laser action.

5.2 Speckle formation

When laser light strikes a white wall or just some surface in space, a speckle pattern is observed. An example is given in figure 5.3.
This phenomenon is not observed with light from a spectral lamp so it must be a special property of laser light. The special coherence properties of laser light lead to the appearance of speckle patterns. The light scattered from the rough surface sets up a complicated, standing wave field in space because of the high coherence of the light. By interference of the light waves coming from different points of the surface there are statistically distributed field amplitudes and thus also field intensities at different points in space.

5.2.1 Intensity statistics

When looking at a speckle pattern darker parts obviously occur more often than bright spots. The intensity statistics of a speckle pattern requires a coherent scalar light field and assuming that the speckle pattern is generated by scatter-

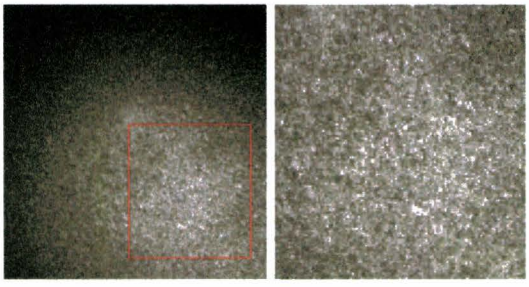

***Fig. 5.3**: A speckle pattern consisting of brighter and darker spots. The right image is a magnification of the red-boxed part of the left image.*

ing of the wave at a rough surface. Each point of the surface can be viewed as a source of spherical waves, with another phase due to the rough surface. The coherence of the light implies the phase difference between two arbitrary points is fixed.
Speckle appears in a signal when that signal is composed of a multitude of independently phased additive complex components (i.e. components having both an amplitude and a phase). The components may have both random lengths (amplitude) and random directions (phases) in the complex plane. When these components are added together, they constitute what is known as a "random walk" [3]. Then the probability density $p(I)$ is given by:

$$p(I) = \frac{1}{\langle I \rangle} \exp\left(-\frac{I}{\langle I \rangle}\right). \tag{5.2}$$

Which shows mathematically that intensities near zero (dark spots) occur more often. Because when I is small the exponent in equation 5.2 becomes large which results in a bigger chance. The standard deviation $\sigma(I)$ of the distribution $p(I)$ in polarized speckle patterns is [8]:

$$\sigma_I^2 = \langle I^2 \rangle - \langle I \rangle^2 = \langle I \rangle^2. \tag{5.3}$$

The standard deviation is equal to the mean intensity ($\sigma = \langle I \rangle$), which means that there is a fully modulated speckle pattern. The probability density function $p(I)$ for white light is a delta-function positioned at the $\langle I \rangle$ value:

$$p(I) = \delta\left(I - \langle I \rangle\right). \tag{5.4}$$

In this case the same (homogeneously distributed) intensity is measured at each point, which is completely different from the intensity distribution with coherent light.

5.2.2 Speckle sizes

In a speckle pattern brighter spots, grains of higher intensity, can be spotted. Their sizes are altered in a peculiar way, becoming smaller when the viewer approaches the scattering surface. Normally this is the other way round. This

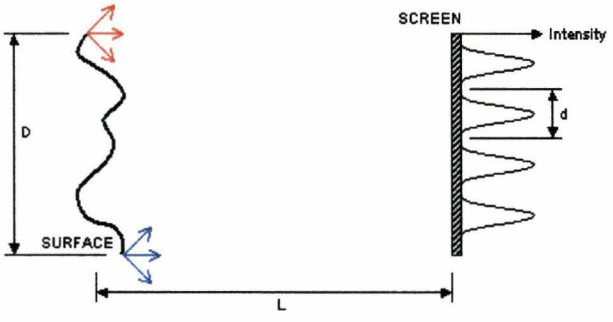

***Fig. 5.4**: Grain size for objective speckle with the interference fringes for the outermost points.*

is explained in more detail next. Take a illuminated area with a diameter D at a distance L from the screen. The separation of the fringes is d, see figure 5.4. Then, by taking two extreme points of the area illuminated, the fringe separation d is obtained:

$$d = \frac{\lambda L}{D}. \tag{5.5}$$

Thus, for a given arrangement, the fringe separation gets larger when the two points approach each other. Since light is radiated from the whole area and not just from the two extreme points, the fringe separation d as given is the smallest speckle size possible. In case of a spherical area of diameter D, d must be corrected by a factor 1.2.

This kind of speckles are called objective speckles, as they are present without further imaging, for instance by the human eye. The other type of speckles called subjective speckles result from a viewing system altering the coherent superposition. This is done by every imaging system and thus every system produces its own speckle size. Using the eye lens to project an image onto the retina, speckles are always seen subjectively.

Objective speckles can only be determined instrumentally. Subjective speckles can be interpreted as a special kind of objective speckles, for any imaging with coherent light introduces them. This can be shown by taking an imaging geometry as depicted in figure 5.5.

Waves of virtually all directions pass the aperture D of the lens. Coming from a rough surface, neighboring waves have a statistical, although fixed, phase difference with respect to each other. Therefore the emitting plane can be shifted for the rough surface to the aperture D with L' the image distance, instead of L. For the case of a emitting plane in infinity (for example a distant rough wall) whose image is formed in the back focal plane, $L' = f$, f being the focal length of the lens. When the wall is not infinitely distant, L' does not equal the focal length f. This can be seen with the help of the lens equation:

$$\frac{1}{Z} + \frac{1}{L'} = \frac{1}{f}, \tag{5.6}$$

with Z the object distance. Introducing the magnification $V = \frac{L'}{Z}$, the image

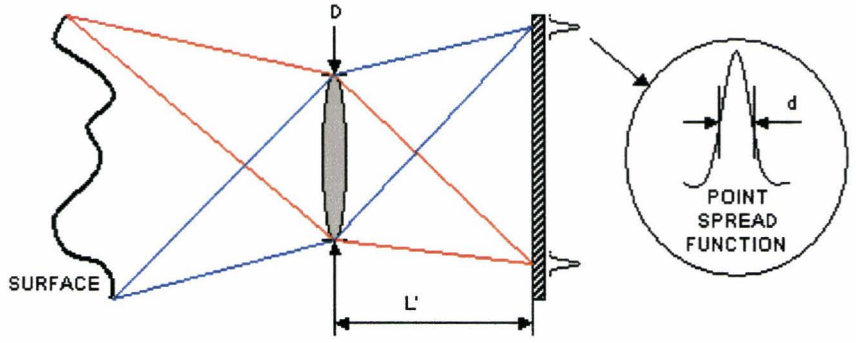

***Fig. 5.5**: Grain size for subjective speckle.*

distance can be obtained:

$$L' = f(V + 1). \tag{5.7}$$

Combining this expression with equation 5.5 together with the F-number (often written as $f/\#$):

$$F = \frac{f}{D}, \tag{5.8}$$

the speckle size is found to be:

$$d = 1.2(1 + V)\lambda F. \tag{5.9}$$

A mixture of objective and subjective speckles is obtained when a coarse speckle pattern is projected onto a screen and is viewed with the eye or a camera.

CCD cameras are useful in recording speckle patterns. In order to obtain reliable results, the following has to be taken into account: CCD cameras have a CCD array that measures the total photon intensity per pixel. A diaphragm can change the camera's F-number. With small F-numbers the speckle size will also be small, according to equation 5.9. But although the speckle is fully modulated, the recorded speckle amplitude will be lower compared to that obtained with large F-numbers. This effect is due to the relative large CCD array pixel size. In case a small F-number is used several speckles will be averaged within one pixel, but when increasing the F-number the speckle size grows and a pixel becomes more and more filled with just one speckle. This leads to an increase of the measured speckle amplitude, see also figure 5.6, where two situations are drawn. The lines in vertical direction represent the border of the pixel. The horizontal lines represent the average intensity measured by the CCD camera whereas the sine-function represents the real speckle pattern. So in the case with the bigger speckles the standard deviation of the measured pixel intensity values will be higher the in the upper case with the small speckles. This results in an increase of the measured speckle amplitude.

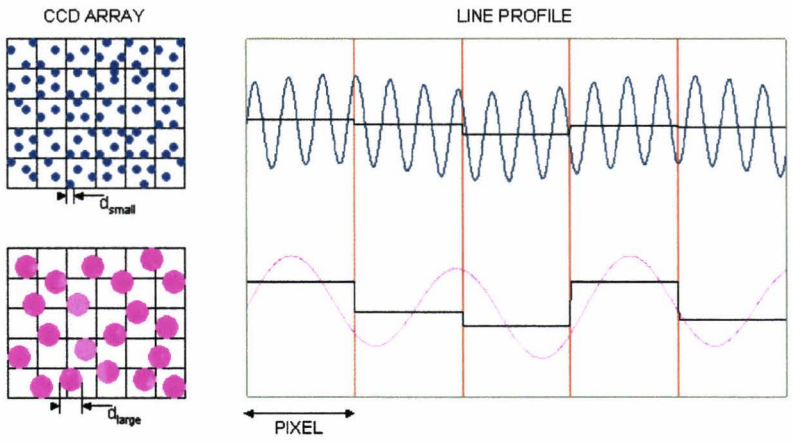

***Fig. 5.6**: A small speckle size leads to a small standard deviation (speckle amplitude). For the several brighter spots will be averaged over the total pixel surface. At larger speckle sizes the number of speckles hitting one pixel surface becomes less, resulting in a larger standard deviation.*

5.3 Speckle reduction methods

There are several solutions proposed to decrease speckle intensity. For example using fast laser pulses, dynamically varying the speckle pattern by vibrating or rotating parts in the optical path or splitting the beam in several beams that are each delayed longer than the coherence length. The most important methods will be discussed in more detail below.

5.3.1 Mirror wobbling

The basic idea of wobbling is to scan a projected image on a screen at small amplitudes, see also figure 5.7. On the one hand, the angle under which the light rays hit the surface changes and additionally, the position at which the light beams hit the screen changes in time. Hence, the emerging speckle pattern changes as well. On the other hand when the scanning angle of the mirror is too large, part of the light beam doesn't hit the surface of the lens, but the surroundings. So a compromise must be made between the speckle reduction and the scanning angle of the mirror.

5.3.2 Mode scrambling

To reduce the spatial coherence of the light, a wave-guide can be used. The resulting effect is the so-called mode scrambling effect. To explain this effect, the propagation of light inside a multi-mode wave-guide is shown in figure 5.8.

When light is coupled to a multi-mode wave-guide at different entrance angles, the light rays propagate through the wave-guide by different paths with different lengths. The fastest track (I), when the light propagates straight through

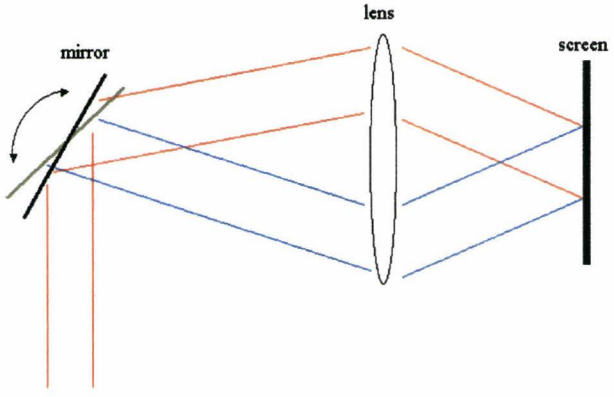

***Fig. 5.7**: The principle of changing the angle of the mirror and thereby the speckle pattern on the screen.*

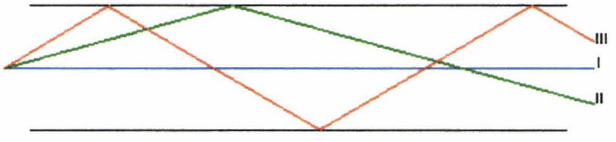

***Fig. 5.8**: Propagation of different modes inside a multi-mode wave-guide.*

the wave-guide, is called the ground mode. When the light rays just fulfill the internal refection condition (III) they travel the longest path possible in the wave-guide. Light hitting the boundary at a larger angle is lost, the rest propagates through the wave-guide following paths of different lengths. If these lengths exceed the coherence length of the laser it leads to speckle reduction. As the coherence length of diode lasers can be in the range of 1 mm, long wave-guides are needed for individual light rays to exceed this coherence length, leading to large set-ups. So a compact device is needed where light has to travel a large distance before leaving. This can be done by using (partial) reflective mirrors.

5.3.3 Rod integrator

A rod integrator shown in figure 5.9 can be made of glass or a transparent plastic.
The entrance plane exists of a high reflective mirror with a small pinhole in it. The better the mirror and the smaller the pinhole (but still $d > 0$) the less light is wasted at the entrance plane. On the other hand not too small else the light cannot enter the integrator. The laser beam must be focused into a very small spot to enter the rod integrator through the pinhole without significant light loss or diffraction effects. When entered the light propagates (by internal reflection) through the rod integrator to the exiting plane. This plane consists of a partly transparent mirror (10% or less) so a small part of the laser beam leaves the rod integrator but most of it is reflected. This part will

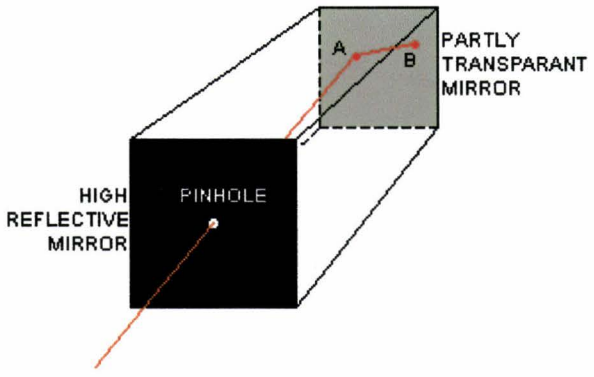

***Fig. 5.9**: A rod integrator. A light beam enters the glass rod through the pinhole, reflects by internal reflection at point A and hits the partly transparent mirror at point B. Only a small part of the beam will be transmitted the rest will be reflected into the rod again.*

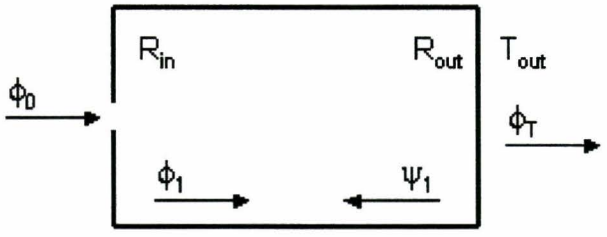

***Fig. 5.10**: The rod integrator with the relevant light fluxes within.*

propagate through the rod integrator for a second time and so on. This way the light leaving the exiting plane is composed of light that passed the integrator a different amount of times. If the coherence length of the laser is smaller than the length of the integrator a speckle reduction is achieved.

Using multiple passes in a rod integrator will result in a decrease of the optical throughput. Light will be lost due to the entrance hole and the not perfect mirror at the entrance plane [4]. The light flux at different positions in the rod integrator is indicated in figure 5.10.

First a light flux, ϕ_0, enters the rod through the pinhole with a relative area r. This flux travels from left to right through the integrator to the exiting plane where ϕ_T is transmitted and the rest is reflected. When hitting the entrance plane, the part that travels through the pinhole will not be reflected and so it is lost. Only the rest of the area, $(1-r)$, will reflect the light with a certain coefficient R_{in}. So the flux ϕ_1 is:

$$\phi_1 = \phi_0 + (1-r)R_{in}\psi_1. \tag{5.10}$$

The flux going from right to left is called ψ_1. Thus after hitting the exiting

plane the back going flux is:

$$\psi_1 = R_{out}\phi_1. \tag{5.11}$$

The transmitted flux is equal to:

$$\phi_T = T_{out}\phi_1. \tag{5.12}$$

Rewriting equation 5.10, 5.11 and 5.12 by eliminating ϕ_1 and ψ_1 gives:

$$\phi_T = \frac{T_{out}\phi_0}{1 - R_{in}R_{out}(1-r)}. \tag{5.13}$$

With equation 5.13 the transmission efficiency of the rod integrator can be calculated:

$$\frac{\phi_T}{\phi_0} = \frac{T_{out}}{1 - R_{in}R_{out}(1-r)}. \tag{5.14}$$

6

Experimental Set-up

In this chapter the optical set-up will be discussed. In the first section for the Computer Generated Holograms and in the second section the set-up for speckle reduction.

6.1 Set-up for displaying Computer Generated Holograms

To be able to create a hologram the following optical parts are needed. First start with a spatially coherent light source, for example a laser. Then a beam expander to enlarge the diameter of this laser beam. The polarizing beam splitter (PBS), reflects the light onto the LCoS micro-display panel. The reflected light from the panel is led through the PBS again where it is transmitted or again reflected. This set-up (real and schematically) is shown in 6.1. In stead of a PBS a beam splitter can be used to create a phase hologram or no splitter at all to be able to get an angle between the panel and beam.
A coherent light source is needed to be able to create a holographic image. Therefore a laser can be used as well as an LED combined with a pinhole [15]. The maximum intensity is reached if a laser is used to lighten the micro-display. The beam has to be increased in diameter to be able to lighten the display as a whole. To achieve this two lenses are used, one with a short focal length in front of one with a larger focal length, separated by a distance equal to the sum of the two individual focal lengths, see figure 6.2. This broadens the beam diameter by the same factor as the factor between the two focal lengths of the two lenses. In this way, the beam remains parallel after passing through this beam expander.
A polarizing beam splitter (PBS) transmits the light with a certain polarization (p-component) and reflects the other part (s-component) of the light to the panel. The panel consists of pixels. Each pixel can be switched between 255 grey levels (8-bit), but this will be simplified by allowing only two states. The reason for doing this is due to the normalization. When normalizing to 255 equal grey steps it will result in having a majority of pixels with the same grey levels. In other words, if a histogram would be made then the majority (more than 90%) of the pixels will have the same few grey levels, resulting in a large peak around the center grey level. This means that the resulting hologram is almost single colored except from a few point. This problem is prevented by

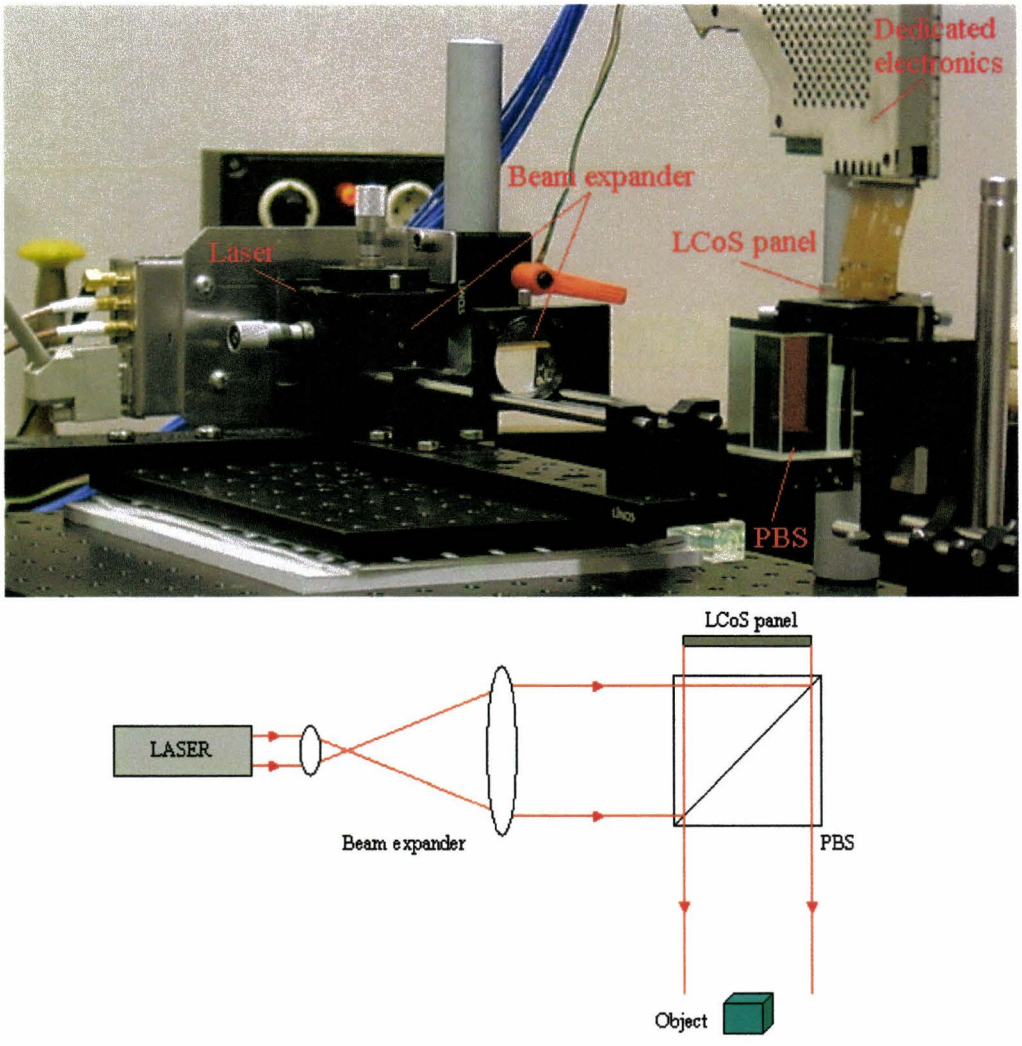

***Fig. 6.1**: The set-up used to produce a holographic image.*

using a binary scale in stead of an 8-bit scale. So a pixel can be turned on or off. In case a pixel is turned on the polarization direction will be altered, in the other case the polarization will be unchanged, more information about the properties of the displays can be found in chapter 4. Depending on the state of the pixel the light will be reflected with either a changed or a unchanged polarization. Next the light is going through the PBS for the second time. Only the light with the changed direction of polarization is going through to form an image in space. The rest will be reflected back to the direction in which the laser light source is located.

After the PBS a lens can be used to filter the zeroth order. In case of filtering, a block is placed at a distance equal to the focal length of the lens to stop the central zeroth order light which is untouched by the interference pattern on the panel. An extra degree of freedom when using a lens is the tunable

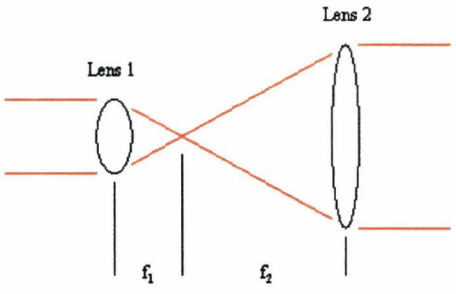

***Fig. 6.2**: A beam expander built from two lenses with different focal lengths.*

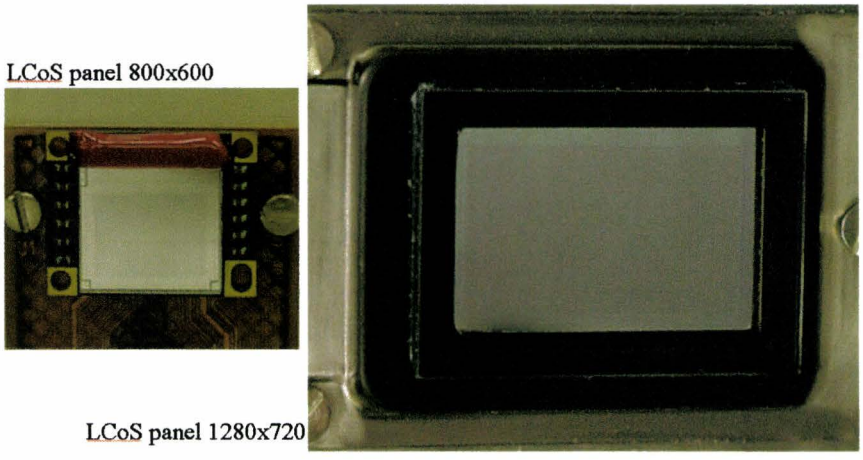

***Fig. 6.3**: The two available LCoS panels. Shown in real proportions, not in real dimensions.*

image distance (depends also on the hologram distance) as well as the coupled magnification.
With off-axis holography the panel is resituated directly into the beam. In stead of the PBS, two different sheets of polarizing material are used to polarize the light. In case of Horizontal Parallax Only (HPO) the standard set-up is used. Only after the PBS a cylindrical lens is placed, with its z-axis in horizontal direction. This means a projection in the vertical direction and only in the horizontal direction the effects of interference.
A thick plastic white screen is used to project the images on. The high intensities make it impossible to look directly into the laser beam not having the eyes damaged. A real object is displayed on the LCoS screen. The LCoS screen is addressed by a PC and dedicated driver electronics. Looking into the beam would result in the object to be created behind the panel, a virtual image. The higher orders will be seen as bright dots which disturb the total image.
Two different LCoS panels are available for experiments, see figure 6.3. A small panel which is 9.5 mm wide and 7.1 mm high, counting 800x600 (0.48M) pixels. The calculated pixel pitch $p = 11.85\mu$m is the smallest one of the two. The

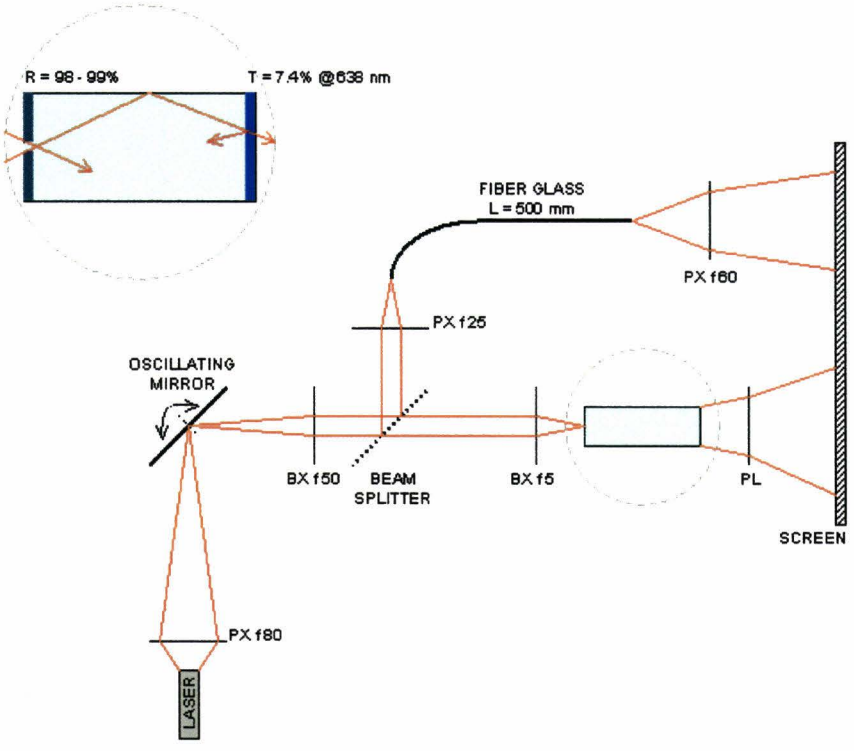

***Fig. 6.4**: The experimental set-up to measure the speckle intensities.*

other panel is 25.5 mm wide and 14.3 mm high, counting 1280x720 (0.92M) pixels. The pitch is $p = 19.89\mu$m. This last mentioned panel had a higher contrast ratio between the on and off state of a single pixel.

6.2 Set-up for speckle reduction

To be able to measure speckle intensities, a laser, some lenses, a screen and a CCD camera are needed. In figure 6.4 our experimental set-up is presented. An image projected on a rough screen being a simple piece of paper, is recorded with a CCD camera. The light rays imaged onto the CCD camera interfere at the CCD array and speckle emerges. The camera with its lens and aperture mimic the human eye with its retina, lens and pupil. The detected signal is transferred to a computer and is analyzed with appropriate software. With this software individual rows or columns can be selected. Speckle is measured by taking a single row or column and then after subtracting the average, the standard variation of the data points is determined. However, due to all sorts of effects (i.e. speckle, intensity profile within the laser beam, diffraction pattern or (dust) particles) the intensity of the profile of this single line is disturbed. Only the intensity differences between pixels on the CCD due to the speckle phenomena are wanted. This means that the recorded intensity profile must be corrected for the above mentioned other effects. For correcting there are

two different methods available: fitting a polynomial function or subtracting a background image. With the first method a polynomial function of a user-defined order is fitted through the measured intensity profile. After dividing the standard deviation, the speckle intensity, is determined. The other possibility is to subtract a background image, an image without the speckle features in it. This background image can be recorded by averaging several recorded images using a vibrating screen while recording. This last method has the advantage that patterns of (dust) particles, the diffraction pattern due to entering through a small pinhole and other irregularities are corrected for. The reproducibility of the measurement was investigated by analyzing several lines and/or columns of the captured image.
Next the oscillating mirror will be discussed. This mirror is used to alter the speckle pattern in time. If the frequency is higher then the integration time of the human eye two or more different speckle patterns are averaged.
The setup contains an oscillating mirror, which can be driven at different frequencies and various voltages leading to various scanning angles. The laser beam is focused on the turning axis of the mirror surface. After hitting the mirror the laser beam is split into two separate beams, the reference signal propagates through a 500 mm long fiberglass before being projected onto the screen [16] and the other propagates through the rod integrator before being projected. This rod integrator, 2 cm long, 1 cm wide and 0.7 cm high, consists of two mirrors; the one with the pinhole ($d = 150\mu$ m) in it reflects 98% of the light, the other transmits 7.4% of the laser beam with a wavelength of 638 nm.

7

RESULTS

In this chapter the results of different experiments will be discussed. Experiments as intensity distribution, on-axis and off-axis imaging, the effects of using a lens and depth of focus are performed and discussed in the next sections.

7.1 Pixel structure of the LCoS panels

Lighting the panel with uniform laser light makes an image of the panel to appear in space. The pixels of the panel are surrounded by a black matrix structure, in other words every light emitting or reflecting part of a pixel is surrounded by a not emitting or reflecting structure. This structure can be seen as a grating with a pitch equal to the pixel-pitch. The angles of the higher order diffractions can be determined by a recorded image at a certain distance. The pixel-pitch can be calculated by knowing the angles of the diffraction orders and then using equation 2.23. Figure 7.1 show a resulting image of an LCoS(800x600) panel illuminated with laser light having such a pixel-structure.

The screen is placed at a distance of 2.31 m. The distance between the zeroth and first order in the horizontal as well as the vertical direction is measured to be 12.3 cm. The same distance in both directions means that the pixels on the panel are squared. Using equation 2.23 the distance d between two adjacent black matrix lines on the panel can be calculated. The angle α is zero because the panel is illuminated perpendicularly. The distance between the lines, which is the pixel pitch, is found to be $d = 11.85\mu$m.

7.2 Intensity distribution

In this section the intensity distributions for different generated grids are discussed.
The intensity distribution has been measured for the LCoS(1280x720) panel which had a higher contrast ratio. These measurements are done with a total black panel without the influence of the black matrix. The panel returned a black screen as it should. With the panel switched to peak white, this results in the black matrix to be the grid that is responsible for the higher order images. The intensities per order are measured using an integrating sphere in which the

light of one order is focused with a lens. The results of this experiment are shown in table 7.1 As an additional experiment, the panel was offered a grid which consisted of a repeating black and white columns of pixels. This means that the black matrix is no longer responsible for the generation of the higher orders, but the grid of black and white columns of pixels. A recording of the generated intensity pattern is shown in figure 7.2. The data are presented in table 7.2. The data of table 7.2 are also represented by the red line in figure 7.3. The envelop (blue line) represents the term $\frac{\sin^2\left(\frac{\pi a}{\lambda}\sin\theta\right)}{\left(\frac{\pi a}{\lambda}\sin\theta\right)^2}$ in equation 2.25 which is due to diffraction by the applied grid. Filling in the known parameters leads to the unknown slit-width which is calculated to be $a = 18.2\mu$m. With a pixel-pitch of $p = 19.89\mu$m this leads to a fill-factor of the LCoS pixels of 84%.

7.3 Holographic imaging

In this section we will discuss the written program which calculates the proper holograms in order to get the image one would like to get. If the angle of the illumination beam is changed with respect to the normal perpendicular to the LCoS direction, extra calculations have to be made. This on-axis and off-axis holography are also discussed in this section. Just as the Horizontal Parallax Only imaging, which demands less computing time.

7.3.1 Algorithm

A computer program has been written to calculate the wanted hologram. The source code is listed in Appendix B, but will be described step by step in this paragraph. The steps of the program are schematically shown in figure 7.4. Before anything is done in the program, a calculation time reduction mechanism is used by creating a cosine look-up table. An array of 256 values is filled with the cosine value of an argument between 0 and 2π. When a cosine has to be calculated it can be looked-up in this array by taking the nearest argument and read out the corresponding value.
The first step in this program is to start reading the input image, this can either be a list of object points having three coordinates, or be a black and white file in .ppm format having the same resolution as the LCoS panel used. These .ppm files have a header containing information about the file format, the color depth and the dimensions of the picture. Then follows a list of numbers. The first number is the red value (for example between 0 and 255) for pixel one. The second number represents the green value of pixel one and the third number represents the blue value of pixel one. Number four, five and six correspond to the red, green and blue values of pixel two, and so on. Because we use only black and white input files, the pixels return $(0, 0, 0)$ or $(255, 255, 255)$. The program starts to read all the information and transfers the values into 2D sub arrays for red, green and blue. Then the 2D arrays are scanned to locate the pixels that are turned white. The positions (x, y) of these pixels are stored and given a user-defined depth value (z-coordinate). All the pixels of one input file are assumed to lie in one z-plane. To be able to get information in other

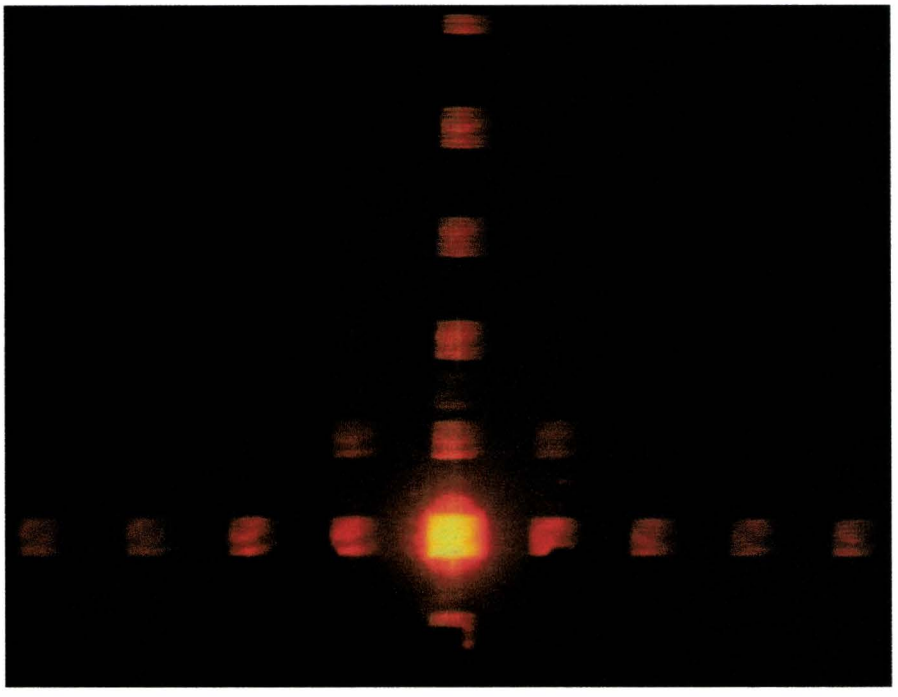

***Fig. 7.1**: The black matrix structure responsible for higher order diffractions.*

***Table 7.1**: The intensities of the light in the different orders when all the pixels of the panel are switched to peak white.*

order	+		−	
0	5600 nA			
1	21.3 nA	0.38%	23.3 nA	0.42%
2	14.9 nA	0.27%	21.3 nA	0.38%
3	10.7 nA	0.19%	11.1 nA	0.20%
4	8.5 nA	0.15%	11.9 nA	0.21%
5	6.3 nA	0.11%	10.2 nA	0.18%
6	4.2 nA	0.08%	6.7 nA	0.12%
7	1.6 nA	0.03%	7.3 nA	0.13%

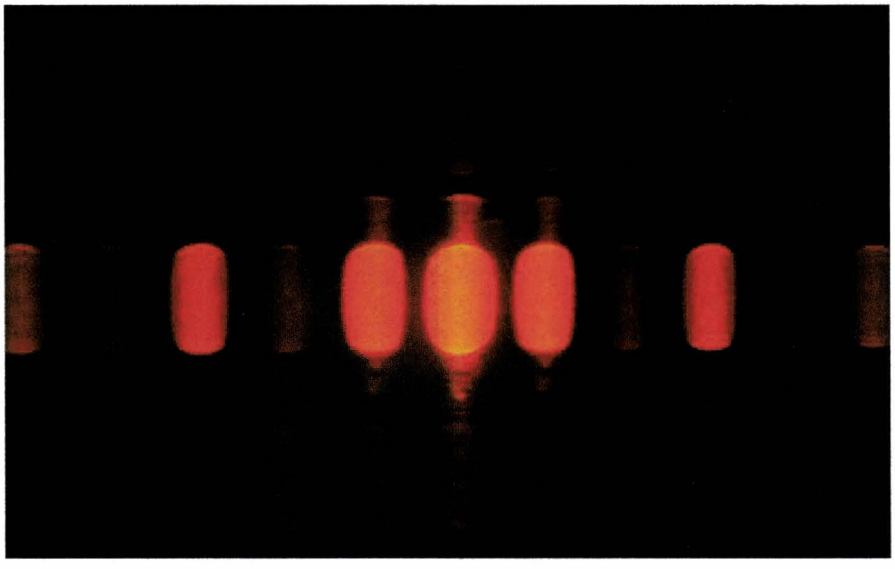

Fig. 7.2: *The higher order diffractions due to a vertical grid.*

z-planes, this procedure of reading an image file has to be repeated. There is a list of coordinates available now, where white pixels are located, whether it was done by reading multiple images or just one, or even user given 3D coordinates. These are the positions where the interference has to be constructive to generate a bright spot at that specific location.

The second step is to calculate the hologram needed to generate the readed image in space. First start with a simple case. Imagine that the image consists of only one white pixel in the middle of the panel at a certain depth value. To be able to calculate the interference pattern at the LCoS panel ($z = 0$), the object beam from the point at $(0, 0, z)$ is needed together with the reference beam. The reference beam is a plane wave with $\phi = 0$ travelling in a direction parallel to the normal of the LCoS panel. The object beam a spherical wave assuming that the point at $(0, 0, z)$ is a point source radiating in all directions. The hologram can be calculated by taking equation 3.4 into account. This hologram, the interference pattern of those two waves at $z = 0$ is known as a Fresnel Zone Plate (FZP). This FZP, see also 3.1, consists of circular rings with their centers marking the (x, y) position of the point and their radii responsible for the z-distance of the point. If an object is built from a lot of points then this procedure with the FZP's can be repeated. However if there are a lot of points in the same z-plane the radii of the rings will not change. The pattern will be translated in the (x, y) direction to set the centers of the rings equal to the position where the point is wanted. This means that if the FZP is calculated for a surface four times as big as the panel its surface, that this FZP can be translated towards every corner of the LCoS panel still providing data for all the pixels of the panel. Calculating this large FZP pattern has the advantage that it has to be done only once. For all other points at the same z-distance the pattern has to be shifted only. By knowing all the (x, y) positions of the white

Table 7.2: *The intensities of the light in the different orders when the panel is filled with a grid of black and white vertical pixel rows.*

order	+		−	
0	1450 nA			
1	570 nA	39.3%	550 nA	37.9%
2	11.2 nA	0.77%	11.8 nA	0.81%
3	72.2 nA	4.98%	49.0 nA	3.38%
4	12.0 nA	0.83%	7.1 nA	0.49%
5	16.4 nA	1.13%	13.4 nA	0.92%
6	6.7 nA	0.46%	7.2 nA	0.50%
7	7.2 nA	0.50%	8.2 nA	0.57%
8	6.2 nA	0.43%	5.7 nA	0.39%
9	2.9 nA	0.20%	2.3 nA	0.16%
10	4.8 nA	0.33%	3.4 nA	0.23%
11	1.3 nA	0.09%		
12	3.2 nA	0.22%		
13	1.1 nA	0.08%		
14	3.0 nA	0.21%		

pixels, they are determined in the first step of the program, the object can be formed by shifting the FZP and sum them according to equation 3.7. It must be said that the pre-mentioned FZP are in our case not intensity patterns yet, but still arrays representing the ψ-values. Having a closer look at equation 3.7 reveals that there are still some parameters which can be chosen freely. The initial phase of each point. This phase is randomly chosen because it improves the image quality. The initial phase of the reference beam is chosen such that when the real part is taken only a multiplication by unity is left. So in order to get the intensity pattern from our points the cosine (taking the real part) must be taken from all the values. Here the look-up table saves us some time. So now there is the intensity pattern which must be placed on the panel in order to create the points drawn in the input file. But to be able to show the data on the LCoS panel they have to be normalized.

The third step, the normalization is done by scaling all the values calculated for the pixels of the LCoS panel to 2, 4 or 8-bit grey scale. The lowest value is set to zero and the highest value is set to the maximum grey level (1, 15 or 255). Then the values between the minimum and maximum are split into equal domains. The amount of domains depends on the number of grey levels. And then all the values are assigned the number of the domain they are in. Then there is a hologram available coded in grey levels in a two dimensional array ready to be shown on the LCoS panel.

Before displaying, this two dimensional array has to be saved. This is done in the same format as the input file. The header is generated containing the information of the color depth and image size. Then followed by the red, green and blue values per pixel. In our case when working with grey levels only, the

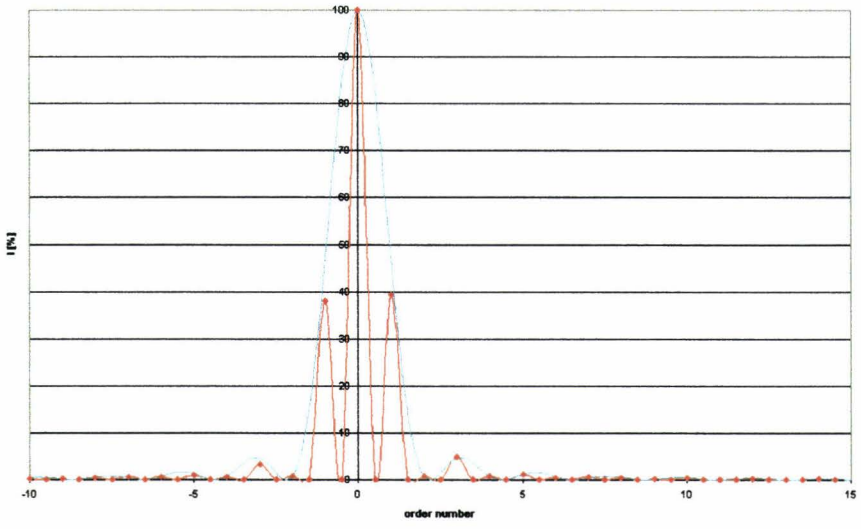

***Fig. 7.3**: The intensity distribution due to a grid on the panel.*

values for red, green and blue for one pixel are the same and all written to the file.
It is easy to change to colored holograms for it is already available in the program. In our set-up a red laser was used so all the calculations are performed with the wavelength of red light. But this can easily be changed to other colors by changing the letter of the color for all the wavelengths are pre-programmed.
A general disadvantage of this method is the long calculation time needed to generate only one hologram. There are a few time reducing mechanisms explored and implemented:

- cosine look-up table [17]; in stead of calculating the cosine function for each pixel every time the value will be looked-up in the table which is filled at the beginning of the calculations.

- calculating the Fresnel Zone Plate only once; if there are more then four object pixels at a same depth then the calculation time will be reduced by calculating the Fresnel Zone Plate once for a surface four times as big. Four times because the pattern should be able to be shifted from the upper-left corner to the lower-right corner and still filling all the pixels with data.

- substituting the square root by using the Fresnel approximation, so instead of using $r_n = \sqrt{(x-x_n)^2 + (y-y_n)^2 + (z-z_n)^2}$ the approximation $r_n = z_n + \frac{1}{2z_n}\left((x-x_n)^2 + (y-y_n)^2\right)$. The square root function takes a relative long time to be calculated. Another time reducing mechanism using recurrent formulas replaces the radius calculations which is performed over and over again for each pixel on the panel. Two neighboring pixel do not differ that much in distance to the object point. When using the recurrent formulas the distance to the object point is calculated

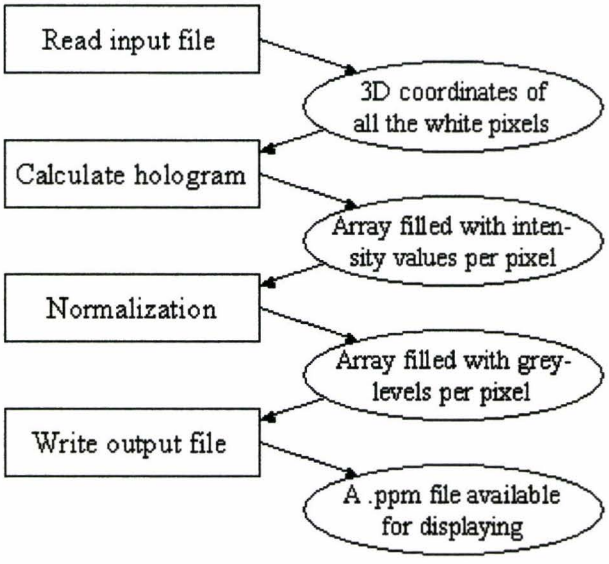

***Fig. 7.4**: The steps taken by the program to calculate a hologram.*

once and then small corrections are added when going to the next pixel on the panel. These formulas can be found in [18] [19] [20] [21]. All the above mentioned mechanisms result in one object point to be calculated in 0.4 s on a Pentium 1.80 GHz processor.

- HPO; this reduces the amount of pixels to be calculated. In stead of a Fresnel Zone Plate in 2D (1280x720 pixels) this pattern has only to be calculated for a 1D line of pixels (1280 pixels). The calculation time for one object point to be calculated is reduced to 0.8 ms.

7.3.2 On-axis imaging

Images can be made if the correct interference pattern is offered to the micro-display panel. The central image (zeroth order) is surrounded by a bright background of light, see figure 7.5 Here we did not block the zeroth order. For this kind of holograms is the algorithm designed described in the previous paragraph.

7.3.3 Off-axis imaging

In figure 7.6 the result from an off-axis image with an on-axis reference beam is displayed. The reference beam is oriented perpendicular to the panel. On this panel the hologram which consists of an extra numerically added grid compared to a hologram which creates an on-axis image. From all the created images on the screen, including the higher order images, there is only one image that is sharp. This is the one located at the angle at which the hologram is calculated.

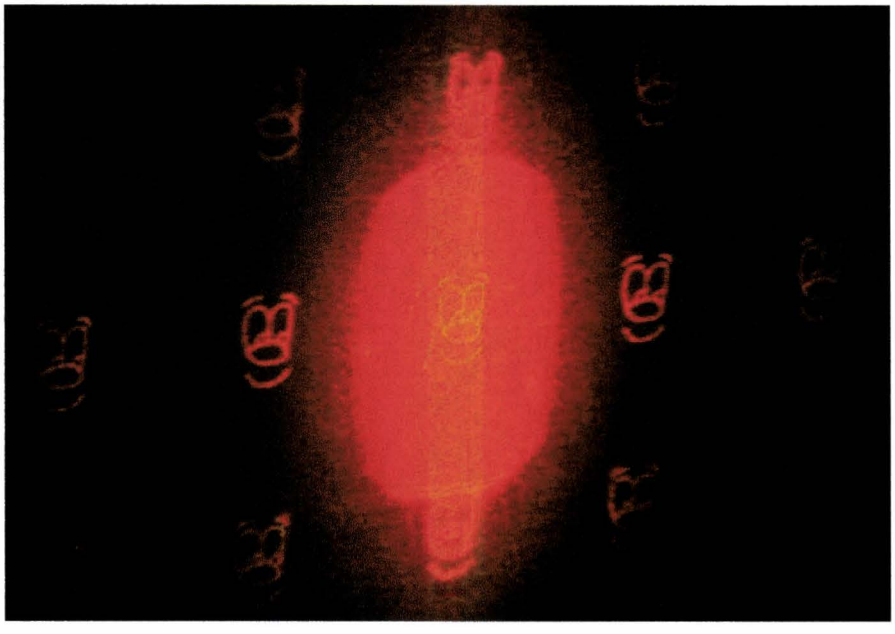

***Fig. 7.5**: A holographic image with bright surrounding light around the center image.*

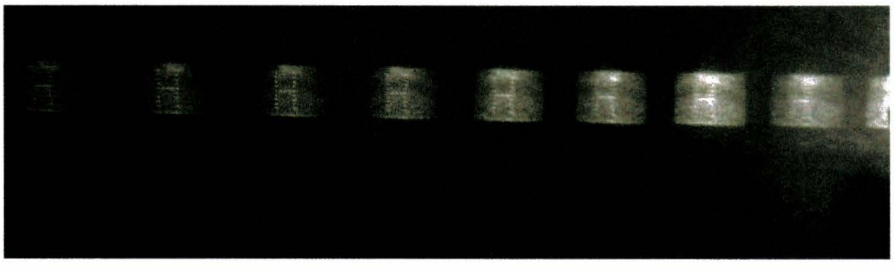

***Fig. 7.6**: Off-axis holographic images with an on-axis reference beam.*

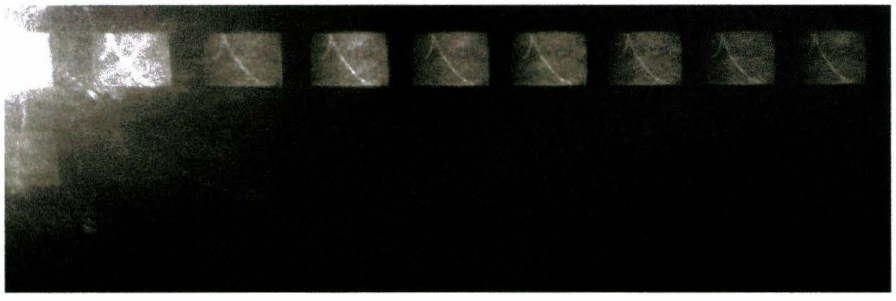

***Fig. 7.7**: On-axis holographic images with an off-axis reference beam.*

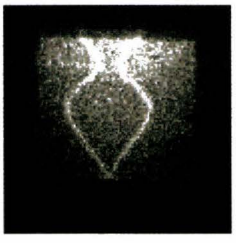

***Fig. 7.8**: An image created with horizontal parallax only.*

The other images have a readable 'H' but the dots forming the image are either elongated in the horizontal or else the vertical direction.

Another way to remove the central spot, the zeroth order, from the image, is to illuminate the panel with a reference beam which had a certain angle according to the normal of the panel. In this case the reference beam cannot be chosen to be a multiplication by unity. Here the multiplication factor will depend on the position at the LCoS panel and the angle of the reference beam, according to equation 3.8. For this reference beam counts that the angle of incidence is also the angle of reflection. The image can still be created perpendicular to the screen. The result of such an image is shown in figure 7.7. A few created images are sharp, the images at wider angles look rather fuzzy. A disadvantage is the low intensity of the images. This can be proven directly from equation 2.19. At large angles, θ becomes larger, which means that the denominator becomes larger and the total intensity less.

7.3.4 Horizontal parallax only imaging

To reduce the calculation time by a factor as large as the number of vertical lines of the panel, the HPO method can be used. In the set-up, a cylinder lens is used to compensate for the loss of holographic information in the vertical direction. In fact, in the vertical direction, a real image is displayed on the panel. This image is projected by the cylinder lens to the same plane as were the holographic image is formed. The image, see figure 7.8, looks grainy. However this is caused by the recording camera.

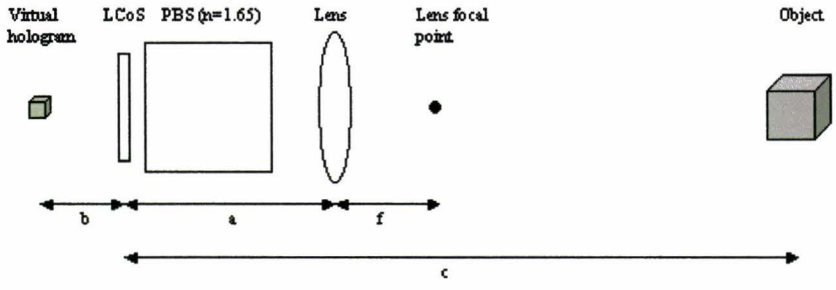

***Fig. 7.9**: The set-up of the different components.*

7.4 The effects of using a lens

A lens can be used to block the zeroth order light beam reflecting directly from the panel. This beam is not affected by the interference pattern on the panel and leads to an unwanted background. Because of the relatively high intensity of the image formed by the interference pattern, a lens can be added to the set-up. This way the zeroth order beam can be focussed to one point and be blocked. But the added lens has more effects on the image formed. The distance from panel to image will be altered by the lens just like the magnification of the image. To determine the effects of an additional lens, a set-up as shown in figure 7.9 is used. The interference pattern put on the LCoS panel generates a holographic image at a distance b in front and behind the panel. A real image as well as a virtual image are created. The lens with a focal length $f$is placed at a distance a in front of the panel. This lens is responsible from the virtual image being imaged to a real holographic image at a distance c in front of the panel. This distance can be calculated using the lens formula, we find

$$c = a + \frac{f(b+a)}{b+a-f} \tag{7.1}$$

The magnification can be calculated knowing the relation between the virtual and the real image.

$$M = \frac{c-a}{b+a} \tag{7.2}$$

The polarizing beam splitter (PBS) is made out of glass and has an other index of refraction than air. A bigger refraction index means a lower speed of light. It takes longer for a light beam to travel across the PBS then through air. Seen in a different perspective this means that the light going through the PBS has to travel a longer distance to reach the finish at the same time compared to a light beam through air.

$$\Delta a = d_{PBS} * (n_{PBS} - 1) \tag{7.3}$$

with d_{PBS} the dimensions of the PBS cube.
The laser beam should be parallel, not converging or diverging, in order to get good results. The set-up is presented in figure 7.9. The hologram is calculated

to create an object after reconstruction at a distance of $b = 0.13$cm. The PBS is cubical with sides which are 2 cm long. The refraction index of this PBS is $n = 1.65$. This elongates the optical path of the light by $\Delta a = 1.3$cm according to the physical path length. The measurement consists of checking equations 7.1 and 7.2 by measuring the distances between the different components and the size of them. Using the equations these distances and the magnification can also be calculated. The results are shown in table 7.3.

***Table 7.3**: The results of the effects of using a lens within the set-up. All figures are given in meters.*

$b = 0.13$, $h_{hol} = 0.006$						
Measured					Calculated	
a	f	h	c	M	c	M
0.113	0.20	0.030	1.24	5.0	1.24	4.7
0.103	0.20	0.038	1.51	6.3	1.51	6.1
0.093	0.20	0.055	2.10	9.2	2.03	8.7
0.163	0.20	0.013	0.80	2.2	0.79	2.2
0.113	0.16	0.011	0.56	1.8	0.58	1.9
0.073	0.16	0.020	0.80	3.3	0.83	3.7

When looking at the distance c where the object should be imaged in focus, the calculated and measured values match within 3%. Remaining errors are mainly due to reading errors. Some distances are difficult to determine, like a for instance. The factors of magnification are not as good as the values for the distances, in this case they match within 10%. This larger variation is due to the large relative error in the size of the hologram h_{hol}, needed to determine the magnification M.

7.5 The effects of a non-parallel illumination beam

A beam expander is used in the set-up to be able to enlarge the beam diameter. The expander consists of two lenses with two different focal lengths. The ratio of these focal lengths is in proportion to the ratio in diameters of the beam before and after. If the distance between the two lenses isn't exactly $f_1 + f_2$, but a bit smaller, not a parallel beam exits the expander, but a divergent beam. The beam can be focussed to a point by placing a lens in the divergent beam. The virtual distance of the light source can be determined using the lens equation after measuring the distance between the focal point and the lens. In case of a parallel beam the focal point is at the same distance as the focal point of the lens itself, so the source distance becomes infinity.
Changing the distance of the light source results in the object being created not at the distance it is calculated for, but further away. in order to measure the effects of a divergent reference beam, two holograms are calculated. One creates an object at 8cm and the other one creates an object at 30cm, both in case of a parallel exposure. The distance of the created object versus the

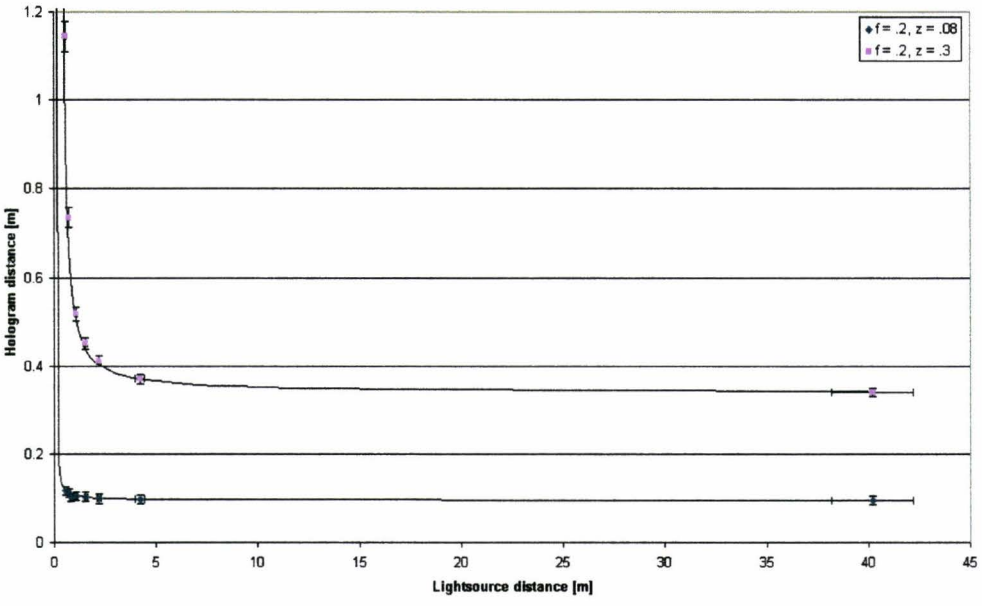

***Fig. 7.10**: The distance of the created object versus the calculated distance of the light source.*

distance of the light source is presented in figure 7.10. As expected the distance of the object is going asymptotically to the 'real' distance using a light source which is going to infinity. The other way around; the distance of the object is going to infinity if the light source is moving towards the focal length of the lens. Using the lens formula the hologram distance is given by $d_{hol} = \frac{d_{source} f}{d_{source} - f}$. In case the hologram was calculated for $z = 0.08$m the focal length found using the fit was found to be $f = 0.095$m. In case the hologram was calculated for $z = 0.3$m the focal length was found to be $f = 0.34$m. The values found are both higher than the actual value, but this can be due to the polarizing beam splitter (PBS). This PBS is a glass cube with a higher refraction index than air and therefore no corrections are made.

7.6 Reconstruction

The first step is to start from an original picture which will be 'translated' into a hologram. This image contains only black, where there is no light wanted, and white where the light should be created, see figure 7.11a.
The original image is placed at a certain (user given) depth and then using our algorithm the hologram is calculated, see figure 7.11b. It is possible to create this hologram in 255 grey levels or in only black and white. Changing the program makes it possible to use more than 255 grey scales.
Taking into account the intensity of the pixel and the corresponding influence onto the phase of the light beam reflected by that same pixel, the reconstruction, also based upon computer simulations, can be made [22] [23]. Several effects are seen. Due to the limited number of pixels of the hologram, a lot of details

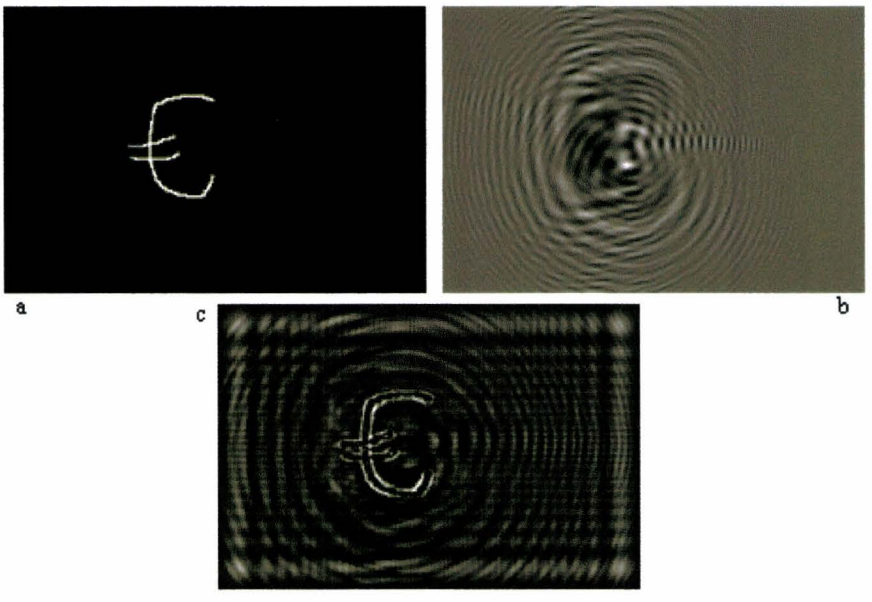

***Fig. 7.11**: From original object (a) via the hologram (b) to the resulting image (c).*

are lost during the conversion, see figure 7.11c. The fringes of the Fresnel Zone Plate for a point object on the display are oscillation too fast for the pixels which are located the furthest away from the point object. Missing these fine structures will lead to less sharp transitions between bright and dark, to be seen at the edges of the euro sign. Also the boxed pattern, clearly to be seen at the edges of the reconstructed image, is due to the limited hologram size.
Assumed is that the phase difference between a black and white pixel corresponds to π. The LC material which generates this phase difference will not necessarily introduce a π-phase difference between a black and white pixel. If this difference should be multiplied by an extra constant this will affect the reconstructed image.

7.7 Depth of focus

For an impression of the depth of focus, a Fresnel Zone Plate which has a focal point at 95 cm from the LCoS panel is displayed on the LCoS panel. Then the intensity profile of the laser beam is measured by placing a screen at a certain distance from the LCoS panel and then record the projected image with a CCD-camera. A few results are shown in figure 7.12.
At 0.71m from the panel the laser beam profile looks rather like a block-function. The fast variations are due to speckle which is automatically generated when coherent laser light reflects off a screen. Coming closer to the focal point of the hologram the intensity profile becomes higher and smaller. Its maximum is around 0.96m where the peak is the smallest and highest. After passing the focal point the profile is not a block-function anymore but a Gaussian-like profile.

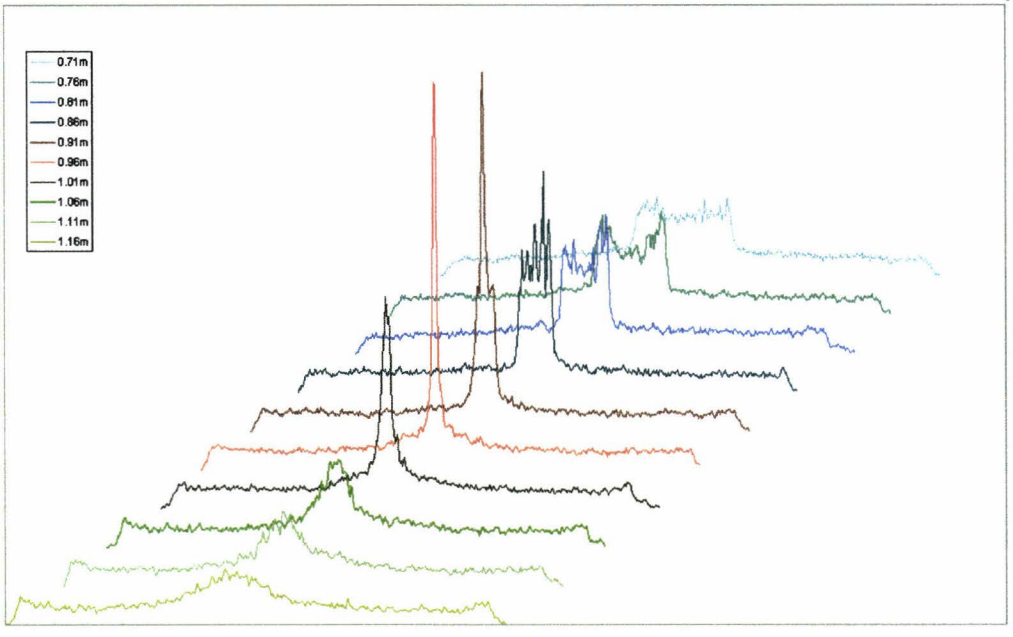

***Fig. 7.12**: The intensity profiles of the laser beam at different distances.*

If the hologram was perfect as well as all the optical components, then this set-up should result in the same point-like image as when using a perfect lens to focus the light beam into a single point. But because the set-up can not be approximated by an ideal lens, the diameter of the spot does not become infinitely small but instead it keeps a certain diameter. This is due to the finite dimensions of the panel, no infinitely small pixels and the finite numerical aperture dimensions. Errors are also induced by a not perfect plane wave leaving the beam expander and lighting the panel.
Expected is a linear dependency of the diameter of the spot on the distance difference Δz between the position of the focus and the position at which the screen is placed.

$$d_1 = c\Delta z \tag{7.4}$$

The d_{eff} is characterized by the FWHM width of the peak in the intensity distribution. This results in the graph presented in figure 7.13. The function fit through the data found is $\sqrt{d_0^2 + d_1^2}$. The constant c is found to be $c = (0.021 \pm 0.005)$.
In the ideal case the surface of the rectangular panel is recalculated to a same area but then round shaped with a certain diameter d_{panel}. Then d_{eff} is given by $d_{eff} = \frac{d_{panel}}{f}\Delta z$. The constant is then found to be $c = \frac{d}{f} = 0.023$. So the results are matching within the error margins.

7.8 Speckle

The effects of speckle must be solved to be able to use a laser light source in a beamer. However, a laser is used in holographic imaging as well, also leading

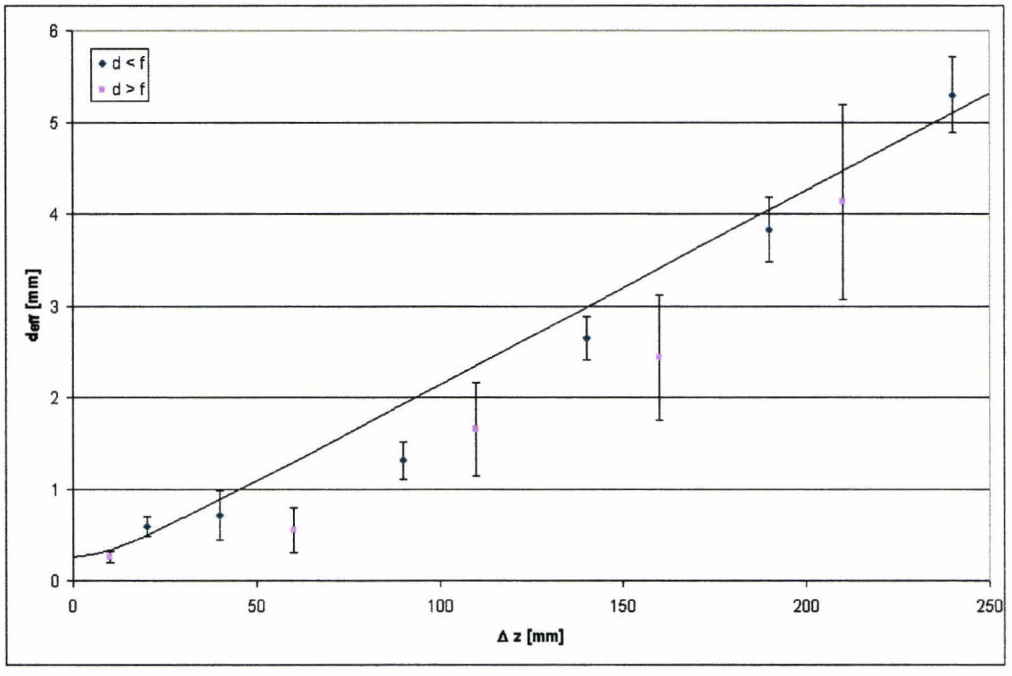

***Fig. 7.13**: The spot diameter versus the difference in distance between the focal point and the position at which the screen is placed.*

to speckle. Compared to using the laser as a light source, the properties of coherence of the laser light are needed in holographic imaging. Therefore the methods which are based on destroying the coherence length of the laser light are not feasible for holographic imaging. The speckle within the desired holographic image can be reduced by using methods like mirror wobbling. This can be done by calculating several holograms with different initial phases of the object points and change the pattern at the panel faster then the integration time of the human eye. Although this does not affect the zeroth order light beam, it works well for the images. Methods to reduce the speckle within the zeroth order light beam can only be based on destroying the coherence of the light, which is on the other hand needed to form the desired interference pattern. For projection purposed this condition is not needed so there a rod integrator can be used to reduce the coherence length of the light.

Some properties of the rod integrator are the transmission factor, the homogeneity of the created image and the speckle intensity within an image of this window. These properties are important because the exit window of the rod integrator is used to illuminate a micro-display panel (with or without an imaging lens between them). The effect of using the oscillating mirror is measured, just as the effects of modulating the laser. The f-number of the laser beam is varied between f/1.4 and f/2.0. This can be calculated using equation 5.8, filling in a laser beam diameter of approximately 3 mm and lens focal distance of 5 mm.

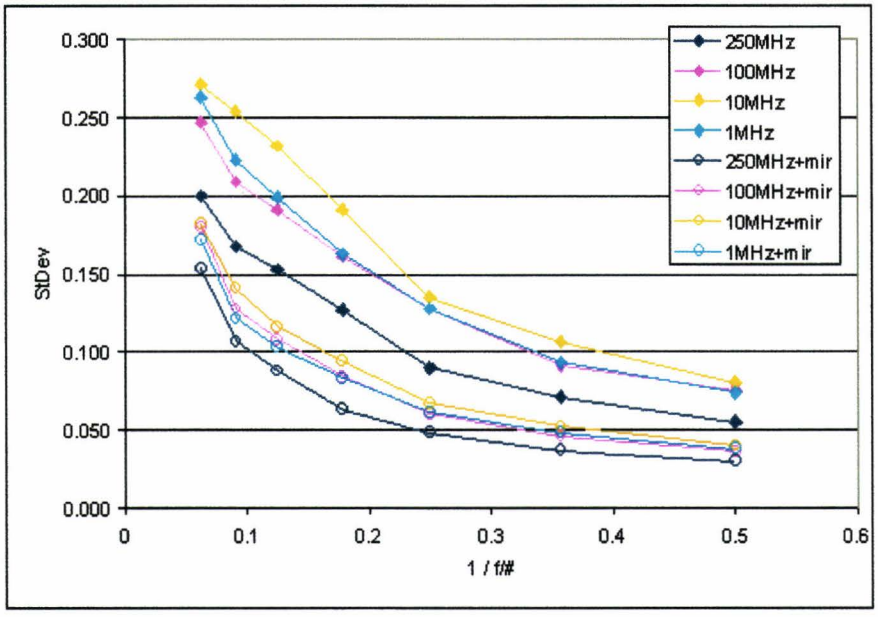

***Fig. 7.14**: The speckle intensity of the reference image created without the rod integrator at different f-numbers of the CCD-camera.*

7.8.1 Oscillating mirror and laser modulation

The oscillating mirror can be driven at various frequencies and voltages. The higher the voltage is, the higher the turning angle of the mirror will be. We used the mirror at 100 Hz and a voltage of 1 V. Then the scanning angle is roughly 20°.

Modulation of the laser, keeping the average power constant, leads to speckle reduction. A shorter pulse means the survival of more modes in the laser cavity leading to a shorter coherence length and so reduction of the speckle intensity. In figure 7.14 the speckle intensity of the created reference image is measured at different f-numbers of the CCD camera. The measurements are performed at different modulation frequencies of the laser and with or without using the oscillating mirror. Using this oscillating mirror decreases the speckle intensity by 45%. Using the laser modulation also helps to lower the speckle amplitude. Modulation at 250 MHz leads to the lowest speckle intensity.

The speckle amplitude is larger when the laser beam is going through the camera lens with a larger f-number. On the other hand the speckle decreases with an increasing laser modulation frequency. Just as using the oscillating mirror is decreasing the speckle amplitude. So both have a beneficial effect on the speckle amplitude.

In figure 7.15 the speckle intensity within the created image is presented. The measurements are again performed at different modulation frequencies of the laser and with of without using the oscillating mirror, but this time the light is guided through the rod integrator.

The speckle amplitude created with the rod integrator is about 50% lower than

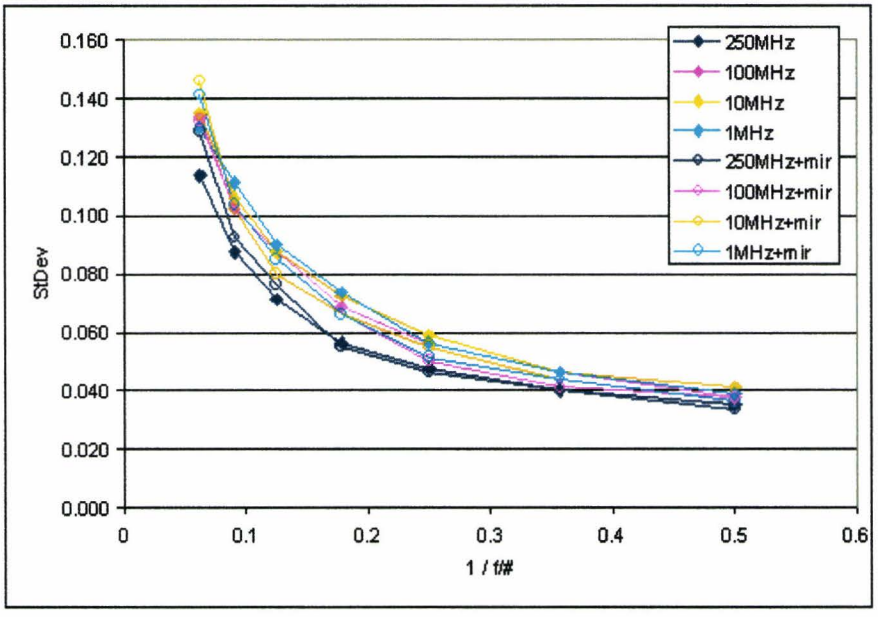

***Fig. 7.15**: The speckle intensity of the reference image created with the rod integrator at different f-numbers of the CCD-camera.*

the reference speckle intensity. But if the oscillating mirror is used the decrease of speckle amplitude is only 10% according to the reference speckle intensity.
It is important to notice that, in combination with the rod integrator, using laser modulation and/or using the oscillating mirror has no significant effect. This means that because of the distance light will have to propagate through the rod integrator, the coherence length of the laser beam is exceeded. By making the integrator shorter it is expected that there will be a certain length where laser modulation and/or oscillating the mirror again starts making a difference. A disadvantage of shortening the integrator is the fact that the bright spot of the first order light beam exiting the integrator becomes smaller and brighter. For there is light entering through the pinhole and exiting the backplane immediately. So the pinhole is projected onto the exit window generating a bright spot. Enlarging the integrator ensures that a large part of the light is reflected off the sides before reaching the exit window of the integrator. The light exiting is distributed more homogeneously. Shortening the integrator will result in just the opposite.
All the above-mentioned speckle intensities are determined by using the polynomial fitting method. Because of the diffraction pattern within the created image more then only speckle is measured this way. Therefore the second method, the subtraction of an image without speckle, is used. The results are presented in table 7.4.
Using the subtraction method leads to smaller speckle intensities as calculated by the fitting method. The lowest speckle, about 2.7%, is measured with laser modulation of 100-250 MHz and without using the oscillating mirror. The speckle intensity measured with the second method but with modulating the

***Table 7.4**: The speckle intensities measured with two different methods.*

$F/1.3$, t_{exp} = 10ms, V_{laser} = 150mV, $V_{oscmirror}$ = 6.1V			
Modulation frequency	250 MHz	100 MHz	10 MHz
With polynomial fit	4.6%	4.4%	4.9%
With image subtraction	2.7%	2.7%	3.0%

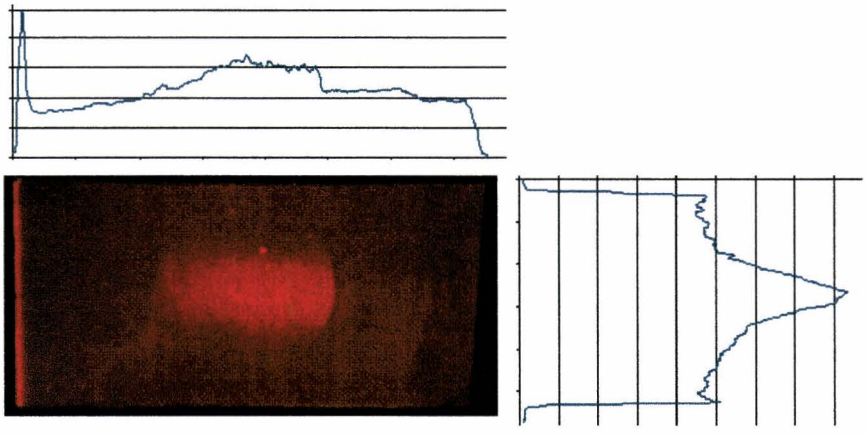

***Fig. 7.16**: The total line or column intensity of a created image using the rod integrator.*

laser is about 4.2% at the same laser power (but then all the time instead of half the time).

Although the speckle amplitude is only 2.7%, it is still clearly visible. It is unknown if this will distort the projected image using a complete beamer set-up, or that it is hardly to be seen.

7.8.2 Homogeneity

An image of the light distribution at the exit window of the rod integrator is shown in figure 7.16.

In the center of the projected image there appears to be a bright spot. This is the part of the laser beam that propagates through the integrator only one time. The sharp edge of the spot can be due to a projection of the pinhole at the entrance plane. Focusing the beam into a smaller spot, or enlarging the radius of the hole, results in a disappearance of this edge, but on the contrary leads to larger intensity differences between the spot and the rest of the image or leads to a larger spot. For a homogeneous image the laser beam must be as divergent as possible, but not too divergent to result in angles beyond the critical angle for total internal reflection. A problem is the clearly visible edge in the created image, so an optimum has to be found.

7.8.3 Transmission factor of the integrator

The throughput of the integrator is measured using an integrating sphere. Measuring the generated current of the photo diode when the rod integrator is part of the optics and divide this value by the measured value when the integrator is no part of the optics leads to the transmission factor. The measured values are presented in table 7.5.

Table 7.5: *The transmission factors calculated at different laser powers.*

Without integrator	With integrator	Transmission
1.83 nA	1.28 nA	0.70
4.10 nA	2.78 nA	0.68
5.65 nA	3.92 nA	0.69
7.36 nA	4.99 nA	0.68
8.80 nA	6.02 nA	0.68
10.39 nA	7.07 nA	0.68
11.80 nA	8.08 nA	0.68
13.27 nA	9.12 nA	0.69
14.84 nA	10.24 nA	0.69
17.50 nA	12.05 nA	0.69

In total room darkness the generated current of the photo diode is 0.38 pA. About 69% of the light propagates through the integrator coming out of the exiting plane. Using equation 5.13 this means a R_{in} of 0.965 instead of the given 0.98 in figure 6.4. The reflection coefficient of the entrance plane can be higher when using a better mirror. In our set-up a reflecting foil is used. Also the semi-transparent mirror on the exiting plane has some irregularities, for example dust particles scattering the light in any direction, which can result in losing light in the proper direction.

8

Conclusions and Recommendations

In this chapter an overview is given of the work done and the most important conclusions drawn from the performed experiments.

8.1 Computer Generated Holograms

First an overview of the experiments performed. Illuminating the LCoS panel results in a diffraction pattern in space. This specific intensity distribution is due to the pixel structure of the panel. Changing the information on the panel a grid can be made resulting in other specific intensity distributions. With alternating black and white columns of pixels, the theoretical distribution is compared to the measured distribution. They match rather well except for the fact that the distance between two white columns is more than twice the width of such a white column. This effect is caused by the black matrix within the LCoS panel, resulting in an inward shift of the intensity peaks due to the interference. Using this shift the fill-factor of our LCoS panel is determined to be 84%.
To be able to create not only grids, but complete images a holographic imaging algorithm has been written. This program makes it possible to calculate on-axis, off-axis and Horizontal Parallax Only (HPO) images. This program also allows for reconstruction. In the ideal case this reconstruction is exactly the same as the image started from, but due to imperfections and limited dimensions there are differences. Furthermore the effects of using a lens are explored, just as the effects of a non-parallel illumination beam. The depth of focus is also measured.
To be able to produce full colored objects three lasers are needed. These lasers have to be synchronized with the video signal sent from the monitor to the panel. In other words to have the right laser on for the correct period of time. When generating an object this should be done as close to the panel as possible. Because the viewing angle is the largest this way. At large distances there is only a small angle within which the created object can be seen. However creating an object close to the panel means large diffraction angles for the pixels at the edge of the panel. To be able to reach these large angles, the fringes have to be very close to each other. In practice there is a minimum distance. The pixel

pitch is the lowest possible fringe distance.
The sizes of the pixels on the LCoS panel do not influence the amount of information which can be displayed. A larger pixel leads to a smaller angle of light spreading due to diffraction, so objects have to be created at larger distances from the panel.
A problem is the normalization at the 255 grey levels if there are a lot of object points. Then there will be a sort of Gaussian profile histogram with a lot of pixels which have a value within the middle 5 grey levels. In other words, there is a small high peak in the histogram to be found at the middle grey levels. The result is a rather uniform grey image which lost its information of the object to be generated. In that case it is better to use the black and white coding, contrary to what one would expect. This must be due to the normalization procedure used.
In spite of the fact that holography offers all the depth cues there are some major disadvantages which make the technology difficult to use in 3D-displays for the time being. These disadvantages will be discussed next.

Panels too small Small panels reduce the distance at which an object can be created. At larger distances the hologram pattern will be coarse and the details are lost for they are falling out of the panel. Larger panels, more pixels, enable the small details to be displayed at the panel as well.

Small viewing angle The closer to the panel the object is created, the larger the viewing angle will be. It can be compared to viewing through a window, standing close to it shows a large, wide view of the environment. But at large distances from the window, only a small part of the environment outside is shown.

Pixel pitch too large The pixel pitch determines the size of the smallest details if an object is created at a fixed distance. A smaller pitch makes it possible to display smaller fringes and these correspond to more detail in the created object. Especially at the edges of the lines, the smaller the fringes are the sharper the transition between dark and bright.

One color For this time the objects created are only red and dark, due to the fact that the only laser used was a red one. Another problem with the laser is the uniformity of the created laser beam. After passing the beam expander the beam is not homogeneous at all. In the center of the beam the intensity is a lot higher as at the edges of the beam. Yet another problem is the zeroth order light beam propagating through the set-up, not being affected by the pattern on the LCoS panel, causing a speckled background around the desired image.

Higher order disturbance Due to the pixel structure (the black matrix structure) on the LCoS panel, higher order images are created. Smaller structures are responsible for higher diffraction angles, thus here also smaller pixels. This allows images to be created closer to the panel because the higher order views are distinguishable from the zeroth order. So that the images of the different orders are not floating into each other.

Large calculation times and high data rates The long computation time is due the amount of calculations which have to be made before the hologram is generated. For every point in the object, for every pixel on the panel the distance has to be calculated, just as the amount of waves that fit within.

Due to all the disadvantages mentioned above holography cannot be implemented as a 3D-display technique at this moment. When it is able to cope with a few disadvantages (or all) then holography results in a very realistic way of showing 3D images. An example which is within the reach of the possibilities for the near future is a single pixel array with a lot of small pixels. By scanning this in the horizontal direction one can built an 3D image. This array of pixels uses only HPO and can be made larger than the common LCoS panels.

8.2 Speckle

For holography the speckle can be reduced by alternating different holograms resulting in the same image but with other initial phases per object point. If a laser source had to be used as a light source, the speckle can be reduced using methods that overcome the coherence length of the laser light. Therefore we have investigated the reduction of speckle by using a so called rod integrator. To lower the speckle, the individual light rays have to travel different distances. When these distances vary more than the coherence length of the light, the beam acts as coming from multiple sources. The rod integrator uses this concept to reduce the speckle amplitude. Experiments showed that the speckle modulation depth is reduced from 5.5% to about 2.7%. The concept of altering the travel distances between the several rays works so well that laser modulation and mirror oscillation doesn't effect the speckle amplitude any more. For these things to take any effect again the length of the integrator can be decreased. Because the coherence length of the other colored lasers is unknown nothing can be said about the effect of laser modulation and mirror oscillation for these colors. When forming an image, the divergence of the light beam must be small to be able to capture all the light within the aperture of the lens positioned after the integrator's exiting plane. The problem however with a small angle is the homogeneity of the generated image. A brighter spot is formed in the middle of the image because a first order goes straight from the pinhole through the integrator to the projection screen. Using a mirror with less losses at the entrance plane can increase the throughput. This way more light is emitted so the image becomes brighter or the laser power can be tuned downwards.

Acknowledgements

In this chapter I would like to show my gratitude towards all the people who helped me finish this work.
Thanks to the group Visual Experiences lead by Toon Holtslag at Philips Natlab this research and my graduation project could be performed. Despite the fact that I had to change the subject I could count on the support from all the group members.
Special thanks go out to my daily supervisor Marcel Krijn. He was always there to support me with ideas, problems, lenses and the message that students do not have that much days off. Especially the last month of my project when I teased Marcel with a lot of pages to have a look at, he gave them back completely written full of suggestions. In our weekly Monday meetings together with Andre Redert I learned the idea behind this research project.
For that I would like to thank Oscar Willemsen as well. For he guided me through the first three months while I was working on the speckle reduction subject.
Furthermore I would like to thank Gerrit Kroesen my supervisor from the Technische Universiteit Eindhoven. When he paid his monthly visits to the Natlab he was always enthusiastic about the work done. Together with his secretary Rina Boom-Van der Velde they arranged all the things necessary for me to be able to succeed finishing this graduation project.
In my first week at the High Tech Campus I was placed in WY 5.24 together with Peter van den Biggelaar, who helped me to learn the Philips mentality. It were his 'Coffee-breaks' who kept the social aspect at a high level. And even after he had moved to the room next door I often walked in to talk about Philips and other daily businesses.
In the same period Maarten Sluijter was also doing his graduation project at the Visual Experiences group. With him I had a lot of discussions about what we would like to do after we would have finished our graduation project. These talks helped me to form a better image of the next step in my career.
Again I would like to thank all the people who helped me to finish this work.

APPENDIX A

DIFFRACTION

A.1 Single slit diffraction

Consider a monochromatic plane wave of wavelength λ incident on a slit of width a. The formula for a wave ψ, travelling radially in the r direction is given by

$$\psi = \int_{slit} \frac{i}{r\lambda} \psi' \exp[-ikr] d_{slit} \tag{A.1}$$

Let the slit be located at the origin, with $(x', y', 0)$ it's coordinates within the slit and $(x, 0, z)$ the coordinates in space where the intensity will be computed. The slit extends form $x' = -\frac{1}{2}a$ to $x' = \frac{1}{2}a$, and from $y' = -\infty$ to $y' = \infty$. Then

$$r = \sqrt{(x-x')^2 + y'^2 + z^2} = z\left(1 + \frac{(x-x')^2 + y'^2}{z^2}\right)^{\frac{1}{2}} \tag{A.2}$$

Assuming the distance to the target to be much larger than the diffraction width on the target (Fraunhofer diffraction), the binomial expansion rule can be used

$$r \approx z\left(1 + \frac{1}{2}\frac{(x-x')^2 + y'^2}{z^2}\right) = z + \frac{(x-x')^2 + y'^2}{2z} \tag{A.3}$$

The $\frac{1}{r}$ in front in equation A.1 has a small contribution to the magnitude of the intensity compared to the exponential factors. Therefore it will be approximated by $\frac{1}{z}$

$$\begin{aligned}
\psi &= \frac{i\psi'}{z\lambda} \int_{-\frac{1}{2}a}^{\frac{1}{2}a} \int_{-\infty}^{\infty} \exp\left[-ik\left(z + \frac{(x-x')^2 + y'^2}{2z}\right)\right] dx'dy' \\
&= \frac{i\psi'}{z\lambda} \exp(-ikz) \int_{-\frac{1}{2}a}^{\frac{1}{2}a} \exp\left[-ik\frac{(x-x')^2}{2z}\right] dx' \int_{-\infty}^{\infty} \exp\left[-ik\frac{y'^2}{2z}\right] dy' \\
&= \psi' \sqrt{\frac{i}{z\lambda}} \exp\left[-ik\frac{x^2}{2z}\right] \int_{-\frac{1}{2}a}^{\frac{1}{2}a} \exp\left[ik\frac{xx'}{z}\right] \exp\left[-ik\frac{x'^2}{2z}\right] dx'
\end{aligned} \tag{A.4}$$

In Fraunhofer diffraction $\frac{kx'^2}{z}$ is small, so $\exp\left[-ik\frac{x'^2}{2z}\right] \approx 1$. The same holds for $\exp\left[-ik\frac{x^2}{2z}\right]$, thus taking $c = \psi'\sqrt{\frac{i}{z\lambda}}$ gives

$$\begin{aligned} \psi &= c\int_{-\infty}^{\infty} \exp\left[-ik\left(z + \frac{xx'}{z}\right)\right] dx' \\ &= c\frac{\exp\left[\frac{ikax}{2z}\right] - \exp\left[\frac{-ikax}{2z}\right]}{\frac{2ikax}{2z}} \end{aligned} \tag{A.5}$$

Note that $\sin x = \frac{\exp[ix]-\exp[-ix]}{2i}$ and $sin\theta = \frac{x}{z}$, this leads to

$$\psi = c\frac{\sin\left(\frac{ka\sin\theta}{2}\right)}{\frac{ika\sin\theta}{2}} \tag{A.6}$$

Substituting $k = \frac{2\pi}{\lambda}$, the intensity I of the diffracted waves at angle θ is given by

$$\begin{aligned} I(\theta) &= \frac{c}{8\pi}|\psi(\theta)|^2 \\ &= I_0\left(\frac{\sin\left(\frac{\pi a}{\lambda}\sin\theta\right)}{\frac{\pi a}{\lambda}\sin\theta}\right)^2 \end{aligned} \tag{A.7}$$

A.2 N-slit diffraction

In stead of one slit, now consider n slits of size $(a, \infty, 0)$ and spacing d spread along the x'. Generalization is being made by the observation that while y and z remain the same, x' shifts by

$$x'_{j=0,\ldots,n-1} = x'_0 - jd \tag{A.8}$$

To be able to calculate the intensity at an arbitrary point in space the influences of all the slits have to be summed. Following the same steps as with the single slit case, this will lead to

$$\psi = I_0\left(\frac{\sin\left(\frac{\pi a}{\lambda}\sin\theta\right)}{\frac{\pi a}{\lambda}\sin\theta}\right)^2\left(\frac{\sin\left(\frac{N\pi d}{\lambda}\sin\theta\right)}{\sin\left(\frac{\pi d}{\lambda}\sin\theta\right)}\right)^2 \tag{A.9}$$

Appendix B

Algorithm

```
//h:/data/bqoc000~.cpp
//Rob van der Meulen                                                    30 - 06 - 2005
//=============================================================================
//A program to calculate the interference pattern at the holographic plane.
//=============================================================================

#include  <stdlib.h>   #include <stdio.h>   #include <iostream.h>
#include <fstream.h>   #include  <math.h>   #include <windows.h>
#include    <time.h>
using namespace std;

//*****************************************************************************
//                    DECLARATION OF THE GLOBAL VARIABLES
//*****************************************************************************
const int array_x = 1280; const int array_y = 720;

const float pi2 = 6.28318530717958647692528676655 9;

int hologram[3*array_x][array_y];
int punten[2][1000000]; float
cosinus[256];



//*****************************************************************************
//    FILLS A TABLE WITH 256 ARGUMENTS OF THE COSINE FUNCTION BETWEEN 0..2*PI
//*****************************************************************************
void vulcosinustabel() {
  int i;

  for(i = 0; i < 256; i++)
  { cosinus[i] = cos(i * pi2/256.0); }
}

//*****************************************************************************
//              DETERMINES THE MAXIMUM OF A GIVEN 2D-ARRAY
//*****************************************************************************
// MAXIMUM(DATA-ARRAY)
//*****************************************************************************
float maximum(float theta_totaal[][array_y]) {
  float max;
  int i, j;
```

```
  max = theta_totaal[0][0];

  for(j = 0; j < array_y; j++)
  { for(i = 0; i < array_x; i++)
    { if(max < theta_totaal[i][j])
      { max = theta_totaal[i][j]; }
    }
  }

  return max;
}

//*****************************************************************************
//              DETERMINES THE MINIMUM OF A GIVEN 2D-ARRAY
//*****************************************************************************
// MINIMUM(DATA-ARRAY)
//*****************************************************************************
float minimum(float theta_totaal[][array_y]) {
  float min;
  int i, j;

  min = theta_totaal[0][0];

  for(j = 0; j < array_y; j++)
  { for(i = 0; i < array_x; i++)
    { if(min > theta_totaal[i][j])
      { min = theta_totaal[i][j]; }
    }
  }

  return min;
}

//*****************************************************************************
//                MOVES THE CURSOR AT THE OUTPUT SCREEN
//*****************************************************************************
// GOTOXY(HORIZONTAL DISPLACEMENT, VERTICAL DISPLACEMENT)
//*****************************************************************************
void gotoxy(int x, int y) {
  HANDLE hConsoleOutput;
  COORD dwCursorPosition;

  dwCursorPosition.X = x;
  dwCursorPosition.Y = y;
  hConsoleOutput = GetStdHandle(STD_OUTPUT_HANDLE);
  SetConsoleCursorPosition(hConsoleOutput,dwCursorPosition);
}

//*****************************************************************************
// NORMALIZES THE VALUES OF A 2D-ARRAY TO THE NUMBER OF GREY LEVELS (1 OR 255)
//*****************************************************************************
// NORMEER(COLOR (rgb), 1 = BINAIRY OF 255 = GREY LEVELS, NR OF OBJECT POINTS,
//         DATA-ARRAY)
//*****************************************************************************
void normeer(char kleur, int kleurdiepte, int aantalpunten,
             float theta_totaal[][array_y])
```

```
{
  int i, j, bereik, som;
  int histogram[1000000] = {0}, counter;
  float temp, max, min, a, halfpointlevel;

  //DETERMINE THE DATA'S MAXIMUM AND MINIMUM THIS DETERMINES THE SCALE OF THE
  //DATA
    max = maximum(theta_totaal);
    min = minimum(theta_totaal);

  //DETERMINE THE MAXIMUM ABSOLUTE VALUE
    if (max > -1.*min)
    { a = max; }
    else
    { a = -1.*min; }
    printf("\na = %f", a);
    temp = 1.0 / a;

  //DEPENDING ON THE COLOR CHOSEN AND THE NUMBER OF GREY LEVELS
  //THE DATA IS TRANSLATED TO GREY LEVELS. IN CASE OF BLACK AND WHITE THE
  //POSITIVE VALUES BECOME WHITE AND THE NEGATIVE VALUES BECOME BLACK.
    if(kleur == 'r')
    { if(kleurdiepte == 1)
      { for(j = 0; j < array_y; j++)
        { for(i = 0; i < array_x; i++)
          { if(theta_totaal[i][j] > 0)
            { hologram[3*i][j] = 255; }
            else
            { hologram[3*i][j] = 0; }
          }
        }
      }
      else
      { for(j = 0; j < array_y; j++)
        { for(i = 0; i < array_x; i++)
          { hologram[3*i][j] = int(kleurdiepte * temp * (theta_totaal[i][j]-min)); }
        }
      }
    }
    else if(kleur == 'g')
    { if(kleurdiepte == 1)
      { for(j = 0; j < array_y; j++)
        { for(i = 0; i < array_x; i++)
          { if(theta_totaal[i][j] > 0)
            { hologram[3*i+1][j] = 255; }
            else
            { hologram[3*i+1][j] = 0; }
          }
        }
      }
      else
      { for(j = 0; j < array_y; j++)
        { for(i = 0; i < array_x; i++)
          { hologram[3*i+1][j] = int(kleurdiepte * temp * (theta_totaal[i][j]-min)); }
        }
      }
    }
```

```
    else if(kleur == 'b')
    { if(kleurdiepte == 1)
      { for(j = 0; j < array_y; j++)
        { for(i = 0; i < array_x; i++)
          { if(theta_totaal[i][j] > 0)
            { hologram[3*i+2][j] = 255; }
            else
            { hologram[3*i+2][j] = 0; }
          }
        }
      }
      else
      { for(j = 0; j < array_y; j++)
        { for(i = 0; i < array_x; i++)
          { hologram[3*i+2][j] = int(kleurdiepte * temp * (theta_totaal[i][j]-min)); }
        }
      }
    }
}

//*****************************************************************************
//                  READ THE TO BE CREATED IMAGE FROM THE FILE
//*****************************************************************************
// LEES(FILENAME, COLOR OF THE OBJECT POINTS (RGB))
//*****************************************************************************
int lees(char *bestandsnaam, char kleur) {
  int x, j, k, max_x, max_y, kleurdiepte, pixel[3], kleurcode;
  char tijdelijk[50], EndChar[2];

  x=0;

  //DETERMINES THE COLOR OF THE ORIGINAL OBJECT
    if(kleur == 'r')
    { kleurcode=0; }
    else if(kleur == 'g')
    { kleurcode=1; }
    else if(kleur == 'b')
    { kleurcode=2; }

  //OPEN THE FILE WITH THE GIVEN FILENAME
    FILE *fp;
    fp = fopen(bestandsnaam, "r");

  //READ THE HEADER OF THE FILE
    fscanf(fp, "%s\n", &tijdelijk);
    fscanf(fp, "# %s%c", &tijdelijk, &EndChar);
    while (EndChar[0] != '\n')
    { fscanf(fp, " %s%c", &tijdelijk, &EndChar); }
    fscanf(fp, "%i %i\n", &max_x, &max_y);
    fscanf(fp, "%i\n", &kleurdiepte);

  int array[max_x][max_y];

  //READ THE ENTIRE FILE AND FILL THE ARRAY
    for(j = 0; j < max_y; j++)
    { for(k = 0; k < max_x; k++)
      { fscanf(fp, "%i %i %i", &pixel[0], &pixel[1], &pixel[2]);
```

```
        array[k][j] = pixel[kleurcode];
      }
    }

  //CLOSE THE FILE
    fclose(fp);

  //DETERMINE THE X AND Y POSITIONS OF THE WHITE PIXELS AND SAFE THEM IN 'PUNTEN'
    for(j = 0; j < max_y; j++)
    { for(k = 0; k < max_x; k++)
      { if(array[k][j]!=0 && x < 1000000)
        { punten[0][x] = k;
          punten[1][x] = j;
          x++;
        }
      }
    }

  //RETURN THE AMOUNT OF WHITE PIXELS
  return x;
}

//*****************************************************************************
//                            WRITES THE IMAGE TO A FILE
//*****************************************************************************
// SCHRIJF(FILENAME (OVERWRITES IN CASE OF ALREADY EXISTING FILENAME))
//*****************************************************************************
void schrijf(char *bestandsnaam) {
  int j, k;

  //OPENS THE FILE WITH THE GIVEN FILENAME
    FILE *fp;
    fp = fopen(bestandsnaam, "w");

  //WRITES THE HEADER TO THE FILE
    fprintf(fp, "P3\n");
    fprintf(fp, "# Created by R vd Meulen\n");
    fprintf(fp, "%4i %4i\n", array_x, array_y);
    fprintf(fp, "255\n");

  //WRITES THE ARRAY HOLOGRAM[][] TO THE FILE. A WHITE HOLOGRAM IS WRITEN BY
  //WRITING THE SAME VALUE AT THE DIFFERENT COLOR POSITIONS (RGB)
    for(j = 0; j < array_y; j++)
    { for(k = 0; k < 3*array_x; k=k+3)  //schrijf een wit hologram weg (+3)
      { fprintf(fp, "%4i", hologram[k][j]);
        fprintf(fp, "%4i", hologram[k][j]);
        fprintf(fp, "%4i", hologram[k][j]);
      }
      fprintf(fp, "\n");
    }

  //CLOSE THE FILE
    fclose(fp);
}

//*****************************************************************************
//  CALCULATES THE INTERFERENCE PATTERN TO BE ABLE TO CREATE THE WANTED IMAGE
```

```
//*****************************************************************************
// BEREKENHOLOGRAM(COLOR (RGB), SUMMING WITH PREVIOUS IMAGE,
//                 NUMBER OF OBJECTPOINTS, DATA-ARRAY, DEPTH)
//*****************************************************************************
void berekenhologram(char kleur, char optellen, int n_punten,
                                     float theta_totaal[][array_y], float z)
{
  int k, j, l, kk, jj;
    k = 0;
    j = 0;
    l = 0;
  float p, lambda, verschuiving, referentiebundel;
    p = 19.89e-6;  //m
    verschuiving = 0;
    referentiebundel = 0;
  int dotpos_x, dotpos_y;
    dotpos_x  = 0;                dotpos_y  = 0;
  float theta_h[array_x][array_y] = {0.0};
  float theta_tijdelijk[2*array_x][2*array_y] = {0.0};

  srand((unsigned)time(NULL));

  //IN CASE OF 'N' THEN CLEAR THE ARRAY THETA_TOTAAL[][]
    if(optellen == 'j')
    { }
    else
    { for(j = 0; j < array_y; j++)
      { for(k = 0; k < array_x; k++)
        { theta_totaal[k][j] = 0; }
      }
    }

  //CHOOSE THE CORRECT WAVELENGTH OF THE USED LIGHT
    if(kleur == 'r')
    { lambda = 630e-9;
      gotoxy(0,0);
      printf("Red:       /%i", n_punten - 1);
    }
    else if(kleur == 'g')
    { lambda = 550e-9;
      gotoxy(0,0);
      printf("Green:     /%i", n_punten - 1);
    }
    else if(kleur == 'b')
    { lambda = 480e-9;
      gotoxy(0,0);
      printf("Blue:      /%i", n_punten - 1);
    }

  //CALCULATE THE INTERFERENCE PATTERN FOR TWICE THE SURFACE NEEDED OF A
  //POINT IN SPACE AT THE OPTICAL AXIS WITH A DISTANCE AS GIVEN
    for(j=0; j < 2*array_y; j++)
    { jj=array_y-j;
      for(k=0; k < 2*array_x; k++)
      { kk=array_x-k;
        theta_tijdelijk[k][j]=(sqrt(kk*kk*p*p+jj*jj*p*p+z*z)/lambda -
                                    int(sqrt(kk*kk*p*p+jj*jj*p*p+z*z)/lambda));
```

```
      }
    }

  //FOR EACH WHITE POINT THE INTERFERENCE PATTERN CAN BE SHIFTED AND ADDED.
  //THIS LEADS TO THE WANTED INTERFERENCE PATTERN RESULTING FROM X-PIXELS
    for(l = 0; l < n_punten; l++)
    { dotpos_x = punten[0][l];
      dotpos_y = punten[1][l];
      gotoxy(5,0);
      printf("%6i",l);

    //TO EACH POINT IN SPACE A RANDOM PHASE IS ASCRIBED WITHIN THE DISTANCE
    //OF ONE WAVE WITH A CERTAIN WAVELENGTH
      verschuiving = rand()%1000 / 1000.0;

    //ONLY ADD THE FRACTION OF THE COSINE FUNCTION
      for(j = 0; j < array_y; j++)
      { for(k = 0; k < array_x; k++)
        { theta_totaal[k][j] += cosinus[int(256 *
                  ((theta_tijdelijk[array_x-dotpos_x+k][array_y-dotpos_y+j] +
                  1.0 * verschuiving) -
                  int(theta_tijdelijk[array_x-dotpos_x+k][array_y-dotpos_y+j] +
                  1.0 * verschuiving)))]; }
      }

    }

    //NORMALIZE THE DATA ONTO A 0..1 OF 0.255 SCALE TO BE SHOWN ON THE DISPLAY
      normeer(kleur, 1, n_punten, theta_totaal);
}

//*****************************************************************************
//                              MAIN PROGRAM
//*****************************************************************************
void main() {
  float theta_tot[array_x][array_y];// = {0.0};
  time_t starttijd, eindtijd;
  int n_punten, i, j;
  float min, sec;

  //DETERMINE THE STARTING TIME OF THE PROGRAM
    time (&starttijd);

  //FILL THE TABLE
    vulcosinustabel();

  //READ THE OBJECT FILE
    n_punten = lees("1280x720-ring.ppm",'r');

  //CALCULATE THE INTERFERENCE PATTERN (COLOR, ADD IMAGE OR NOT, NUMBER OF POINTS,
  // ARRAY, DEPTH)
    berekenhologram('r', 'n', n_punten, theta_tot, 2.00);

  //WRITE THE HOLOGRAM TO THE GIVEN PPM FILE
    printf("\n\nStart writing file");
    schrijf("hologram-ring-1280x720-200-zw.ppm");
    printf("\nWriting finished\n");
```

```
  //DETERMINE THE FINISHING TIME OF THE PROGRAM AND CALCULATE THE TIME USED TO
  //CALCULATE THE HOLOGRAM
    time (&eindtijd);
    sec = difftime(eindtijd,starttijd);
    min = 1.0*int(sec/60.0);
    sec = sec - 60.0*min;
    printf("Total calculation time: %3.0f minutes %2.0f seconds\n", min, sec);
    printf("\nDone");
    cin.get();
}
```

Bibliography

[1] M.W. Halle. *Multiple Viewpoint Rendering for Three-Dimensional Displays.* PhD thesis, 1997.

[2] S. Pastoor and M. Wöpking. 3-d displays: A review of current technologies. http://www.dgp.toronto.edu/ gf/research/.

[3] C. van Berkel, D. Parker, and A. Franklin. Multiview 3d-lcd. *Proceedings of SPIE*, 2653:32–39, 1996.

[4] H.D. Young and R.A. Freedman. *University Physics.* 9nd edition, 1996.

[5] E. Hecht. *Optics.* 4th edition, 2002.

[6] M.V. Klein. *Optics.* 1st edition, 1970.

[7] W. Plesniak. Incremental update of computer-generated holograms. *Optical Engineering*, 46(6):1560–1571, 2003.

[8] P. Hariharan. *Optical holography, principles, techniques and applications.* 2nd edition, 1996.

[9] F.L. Pedrotti and L.S. Pedrotti. *Introduction to optics.* 2nd edition, 1996.

[10] X. Zhang, S. Liu, and C. Liu. Compact hologram display system with led direct illumination. *Proceedings of SPIE*, 4659:211–219, 2002.

[11] M. Heckmeier, G. Lüssem, K. Tarumi, and W. Becker. *Liquid Crystals for Active Matrix Displays.*

[12] K. Choi, H. Kim, and B. Lee. Full-color autostereoscopic 3d display systeem using color-dispersion-compensated synthetic phase holograms. *Optics Express*, 12(21):5229–5236, 2004.

[13] T. Ito and K. Okano. Color electroholography by three colored reference lights simultaneously incident upon one hologram panel. *Optics Express*, 12(18):4320–4325, 2004.

[14] M. Busker. New speckle reduction mechanisms for laser projection displays. *Philips Research Eindhoven*, PR-TN-2004/00379, 2004.

[15] T. Ito. Holographic reconstruction with a 10-μ m pixel-pitch reflective liquid-crystal display by use of a light-emitting diode reference light. *Optics Express*, 27(16):1406–1408, 2002.

[16] B. Dingel, S. Kawata, and S. Minami. Speckle reduction with virtual incoherent laser illumination using a modified fiber array. *Optik*, 94(3):132–136, 1993.

[17] M. Lucente. Interactive computation of holograms using a look-up table. *Journal of Electronic Imaging*, 2(1):28–34, 1993.

[18] C. Petz and M. Magnor. Fast hologram synthesis for 3d geometry models using graphics hardware. *Proceedings of SPIE*, 5005, 2003.

[19] T. Shimobaba and T. Ito. An efficient computational method suitable for hardware of computer-generated hologram with phase computation by addition. *Computer Physics Communications*, 138:44–52, 2001.

[20] T. Shimobaba, S. Hishinuma, and T. Ito. Special-purpose computer for holography horn-4 with recurrence algorithm. *Computer Physics Communications*, 148:160–170, 2002.

[21] T. Ito and T. Shimobaba. One-unit system for electroholography by use of a special-purpose computational chip with a high-resolution liquid-crystal display toward a three-dimensional television. *Optics Express*, 12(9):1788–1793, 2004.

[22] M. Koenig, O. Deussen, V. Padur, and T. Strothotte. Visualization of hologram reconstruction. *Proceedings of Visual Data Exploration and Analysis VIII*, 4302:80–87, 2001.

[23] L. Yu, Y. An, and L. Cai. Numerical reconstruction of digital holograms with variable viewing angles. *Optics Express*, 10(22):1250–1257, 2002.